

# A Regulatory Module Controlling Pharyngeal Development and Function in *Caenorhabditis elegans*

David S. Fay,<sup>1</sup> Stanley R. G. Polley, Jujiao Kuang, Aleksandra Kuzmanov, James W. Hazel,  
Kumaran Mani, Bethany L. Veo, and John Yochem

Department of Molecular Biology, College of Agriculture and Natural Resources, University of Wyoming, Laramie, Wyoming 82071

**ABSTRACT** In *Caenorhabditis elegans*, the differentiation and morphogenesis of the foregut are controlled by several transcriptional regulators and cell signaling events, and by PHA-1, an essential cytoplasmic protein of unknown function. Previously we have shown that LIN-35 and UBC-18-ARI-1 contribute to the regulation of *pha-1* and pharyngeal development through the Zn-finger protein SUP-35/ZTF-21. Here we characterize SUP-37/ZTF-12 as an additional component of the PHA-1 network regulating pharyngeal development. SUP-37 is encoded by four distinct splice isoforms, which contain up to seven C2H2 Zn-finger domains, and is localized to the nucleus, suggesting a role in transcription. Similar to *sup-35*, *sup-37* loss-of-function mutations can suppress both LOF mutations in *pha-1* as well as synthetic-lethal double mutants, including *lin-35*; *ubb-18*, which are defective in pharyngeal development. Genetic, molecular, and expression data further indicate that SUP-37 and SUP-35 may act at a common step to control pharyngeal morphogenesis, in part through the transcriptional regulation of *pha-1*. Moreover, we find that SUP-35 and SUP-37 effect pharyngeal development through a mechanism that can genetically bypass the requirement for *pha-1* activity. Unlike SUP-35, SUP-37 expression is not regulated by either the LIN-35 or UBC-18-ARI-1 pathways. In addition, SUP-37 carries out two essential functions that are distinct from its role in regulating pharyngeal development with SUP-35. SUP-37 is required within a subset of pharyngeal muscle cells to facilitate coordinated rhythmic pumping and in the somatic gonad to promote ovulation. These latter observations suggest that SUP-37 may be required for the orchestrated contraction of muscle cells within several tissues.

ORGAN development is a complex process that is dependent on the tight spatiotemporal coordination of signaling networks, transcription factors, and effectors of cellular morphogenesis. In *Caenorhabditis elegans*, the foregut, which includes the buccal cavity, pharynx, and intestinal valve cells, has proven to be a powerful model for studies of the molecular mechanisms controlling organogenesis (Mango 2007, 2009). Although containing only 95 nuclei in the adult, the foregut is composed of seven distinct but functionally integrated cell types, which arise from diverse embryonic lineages (Albertson and Thomson 1976; Sulston *et al.* 1983). Furthermore, through autonomous

control, the pharynx is capable of producing a rapid and regular pumping action that is essential for the ingestion and mechanical breakdown of food.

LIN-35/Rb, the *C. elegans* retinoblastoma-family ortholog, and UBC-18/UBCH7-ARI-1/AR1H1, a conserved E2-E3 ubiquitin-modification complex, function redundantly to control an early step of pharyngeal morphogenesis, termed reorientation (Fay *et al.* 2003; Qiu and Fay 2006). At this stage during normal development, the anteriormost cells of the pharyngeal primordium change from a radial configuration (with alignment along the rostrocaudal axis) to a parallel orientation, relative to the dorsoventral axis of the embryo (Portereiko and Mango 2001). At the same time, the apico-basal polarities of the leading anterior cells shift from 30° to 90° to align their axes with the dorsoventral axis. These morphological changes ultimately facilitate the formation of a contiguous epithelial tube composed of pharyngeal cells and cells of the future buccal cavity (mouth). Misexecution of this step leads to a failure of the pharynx to attach to the

Copyright © 2012 by the Genetics Society of America  
doi: 10.1534/genetics.112.140814

Manuscript received March 29, 2012; accepted for publication April 25, 2012  
Supporting information is available online at <http://www.genetics.org/content/suppl/2012/04/27/genetics.112.140814.DC1>.

<sup>1</sup>Corresponding author: Department 3944, 1000 E. University Ave., Department of Molecular Biology, College of Agriculture and Natural Resources, University of Wyoming, Laramie, WY 82071. E-mail: [davidfay@uwyo.edu](mailto:davidfay@uwyo.edu)

buccal cavity (the *Pun* phenotype, for Pharynx unattached), together with concomitant defects in pharyngeal elongation (Fay *et al.* 2003; Portereiko *et al.* 2004).

We recently proposed a mechanism to account for the role of **LIN-35** and **UBC-18-ARI-1** in pharyngeal development (Mani and Fay 2009). Specifically, **LIN-35** and **UBC-18-ARI-1** mutually inhibit the expression of **SUP-35/ZTF-21**, a Zn-finger protein. In the case of **LIN-35**, repression of **SUP-35** occurs at the level of transcription and is carried out in conjunction with members of an evolutionarily conserved transcriptional repressor complex that contains E2F (Fay *et al.* 2004; Fay and Yochem 2007; van den Heuvel and Dyson 2008). In contrast, **UBC-18-ARI-1** inhibits **SUP-35** post-transcriptionally, most likely at the level of protein stability, through ubiquitin-mediated proteolysis (Mani and Fay 2009). **SUP-35** in turn functions to transcriptionally repress the expression of **PHA-1**, a novel protein required for pharyngeal development (Schnabel and Schnabel 1990; Granato *et al.* 1994a; Fay *et al.* 2004). Thus, in *lin-35*; *ubb-18* double mutants, **SUP-35** protein levels are elevated because of the loss of two negative regulators, which leads to a reduction in **PHA-1** and subsequent defects (Mani and Fay 2009).

Consistent with this model, loss of **SUP-35** activity can suppress the synthetic lethal phenotype of *lin-35*; *ubb-18* double mutants as well as lethality associated with partial loss-of-function (LOF) alleles of *pha-1* (Mani and Fay 2009). Conversely, overexpression of **SUP-35** in wild-type animals induces pharyngeal defects that phenocopy *pha-1* LOF mutations. Furthermore, pharyngeal defects induced by **SUP-35** overexpression are observed only in the presence of wild-type **SUP-36** and **SUP-37**, and *sup-36* and *sup-37* LOF mutants suppress the synthetic lethality of *lin-35*; *ubb-18* double mutants as well as *pha-1* partial LOF mutations (Schnabel *et al.* 1991; Fay *et al.* 2004; Mani and Fay 2009). These findings link **SUP-35**, **SUP-36**, and **SUP-37** as functional members of a regulatory module involved in the control of pharyngeal development in conjunction with **PHA-1**.

Here we show that **SUP-37/ZTF-12**, a C2H2 Zn-finger protein, acts with **SUP-35** to control pharyngeal development in part through the regulation of *pha-1*. However, newly acquired genetic data using null alleles of *pha-1* demonstrate that the relationship between **PHA-1**, **SUP-35**, and **SUP-37** must also involve a mechanism that is independent of *pha-1* transcriptional regulation. We also find that, in addition to its role in pharyngeal development, **SUP-37** functions independently of **SUP-35** to regulate two essential processes that share a common feature of involving the coordinated contraction of muscle cells.

## Materials and Methods

### Strains and maintenance

*C. elegans* strains were maintained using standard procedures (Stiernagle 2005). Strains used in this study include GE24 [*pha-1(e2123ts)* III], WY83 [*lin-35(n745)* I; *ubb-18*

(*ku254*) III; *kuEx119(lin-35+; sur-5::GFP)*], WY119 [*lin-35(n745)* I; *pha-1(fd1)* III; *kuEx119*], WY477 [*ari-1(tm2549)* I; *pha-1(e2123ts)* *dpy-18(e499)* III], WY165 [*pha-1(e2123ts)* III; *sup-37(e2215)* V], GE336 [*pha-1(e2123ts)* *dpy-18(e499)* III; *sup-37(e2214)* V], GE338 [*pha-1(e2123ts)* *dpy-18(e499)* III; *sup-37(e2216)* V], GE339 [*pha-1(e2123ts)* *dpy-18(e499)* III; *sup-37(t1954)* V], GE340 [*pha-1(e2123ts)* *dpy-18(e499)* III; *sup-37(t1955)* V], GE2158 [*tDf2/qc1 dpy-19(e1259) glp-1(q339)* III], DR108 [*dpy-11(e224) unc-42(e270)* V], WY160 [*pha-1(e2123ts)* backcrossed five times to CB4856], WY170 [*pha-1(e2123ts)* III; *dpy-11(e224) unc-76(e911)* V], WY178 [*pha-1(e2123ts)* III; *dpy-11(e224) sup-37(e2215) unc-76(e911)* V], MT14545 [*dpy-11(e224) sup-37(e2215)* V], WY732 [*sup-37(tm1810)* V; *fdEx175 (sup-37+, sur-5::GFP)*], WY733 [*sup-37(tm356)* V; *fdEx174 (sup-37+, sur-5::GFP)*], ZW10430 [*Psup-37::his-24::mCherry*], WY803 [*fdEx176 (Psup-37::sup-37::mCherry)*], and WY835 [*sup-37(tm1083); fdEx176*]. *sup-37* deletion alleles (*tm356*, *tm481*, and *tm1083*) and *pha-1* deletion alleles (*tm3569* and *tm3671*) were obtained from the National BioResource Project (NBRP) Japan and were confirmed by PCR and outcrossed six times prior to any analysis.

### Genetic mapping of *sup-37*

Preliminary mapping placed *sup-37* on LGV linkage group (LG) V (Schnabel *et al.* 1991) (data not shown). To further narrow down the *sup-37* region, three-point mapping was performed using the balanced strain *pha-1(e2123ts); dpy-11 unc-76/sup-37(e2215)*. Of the progeny, 10/49 Dpy non-Unc and 49/50 Unc non-Dpy acquired the *sup-37* mutation. Furthermore, linked three-point mapping using the strain *pha-1(e2123ts); dpy-11 sup-37(e2215) unc-76/+* resulted in 21/29 Dpy non-Unc and 18/32 Unc non-Dpy animals that retained the *sup-37* mutation. For SNP mapping, *pha-1(e2123ts)* hermaphrodites were backcrossed five times into CB4856 Hawaiian males, and the resulting *pha-1(e2123ts); CG4856-5x* males were crossed to *pha-1(e2123ts); dpy-11 sup-37(e2215) unc-76* hermaphrodites, followed by standard SNP mapping procedures (Fay 2006). By analyzing 400 Dpy non-Unc and Unc non-Dpy recombinants, the *sup-37* mutation was narrowed down to an ~300-kb region containing 95 genes between the sequencing SNPs F41E6 at position 10,060 and H14N18 at position 3200 (yy49b05.s1@112,-,59 yy44b04.s1@483,-,33).

### Transgenic *sup-37* rescue experiments

Extrachromosomal arrays containing fosmid WRM0620dH02 (which contains the *sup-37* locus) along with the coinjection marker pTG96 (SUR-5::GFP) (Yochem *et al.* 1998), were initially generated in N2 strains (*fdEx91-94*). Males containing these arrays were then crossed to balanced strains containing the larval-lethal *sup-37* deletion alleles *tm356* and *tm1083*. In subsequent generations, array-containing *tm356* and *tm1083* homozygous strains were isolated and found to be completely rescued for larval lethality by the presence of wild-type *sup-37*. To measure the activity of the *sup-37* arrays in suppression

assays, N2 males carrying arrays were mated to *pha-1* (*e2123ts*) *dpy-18*; *sup-37*(*e2216*) hermaphrodites at 16°. F<sub>1</sub> cross-progeny that carried the array were isolated and allowed to self-fertilize. Thirty *Dpy* L4-stage F<sub>2</sub>'s containing the *sup-37* rescuing array were transferred to 25°, and their progeny were scored for viability. None of the 30 *Dpy* animals produced viable array-positive progeny, whereas about three-fourths produced viable array-minus *Dpy* animals. *sup-37* rescue experiments were further validated using extrachromosomal arrays containing an ~9.5-kb PCR-generated fragment from C01B7.1 (primers: 5'-AGATACACGATAA CTTCCACCC-3', 5'-GCAATATCTGCTCATACAGTGCC-3') containing the complete *sup-37* locus only, as described above.

#### **Genetic analysis of suppression**

To test suppression of *pha-1*(*e2123ts*) mutants by the nonlethal *sup-37*(*tm481*) deletion allele, *pha-1*(*e2123ts*); *sup-37*(*tm481*) double mutants were generated by crossing *pha-1*(*e2123ts*)/+ males to *sup-37*(*tm481*) hermaphrodites at 16°. Cross-progeny animals of the genotype *pha-1*(*e2123ts*)/+; *sup-37*(*tm481*)/+ were identified by Poison-primer PCR for the *tm481* deletion (Edgley *et al.* 2002) and PCR followed by *Bst*1107I digestion for *pha-1*(*e2123*); the *e2123ts* mutation creates a restriction polymorphism and can be assayed by PCR amplification of the mutant region followed by restriction digestion using *Bst*1107I. F<sub>1</sub> cross-progeny were allowed to self-fertilize at 16° for 24 hr, and F<sub>2</sub> animals of the genotype *pha-1*(*e2123ts*); *sup-37*(*tm481*) were identified as described above and tested for growth at 25°. Three independent isolates of *pha-1*(*e2123ts*); *sup-37*(*tm481*) mutants were tested for suppression at both 20° and 25°; none of the isolates produced viable progeny at either temperature and lethal larvae and embryos displayed a Pun phenotype, consistent with a lack of *pha-1* suppression by *sup-37*(*tm481*).

To test for suppression of the *pha-1* null deletion alleles *tm3671* and *tm3569* by *sup-35* and *sup-37*, homozygous *pha-1* strains carrying extrachromosomal arrays containing the *pha-1* rescuing plasmid pBX (Granato *et al.* 1994a), along with the co-injection marker SUR-5::RFP (Yochem *et al.* 1998), were generated. To assay for suppression by *sup-35*, array-rescued *pha-1* deletion mutants were grown on *sup-35*(RNAi) plates and array-negative (RFP<sup>-</sup>) progeny were observed in subsequent generations and further genotyped at the *pha-1* locus by PCR (Mani and Fay 2009). To assay for *sup-37* suppression of the *pha-1* deletions, double mutants of *pha-1* (*tm2569* or *tm3671*) and *sup-37* (*tm356* or *tm1083*) were generated and confirmed by PCR. Moreover, for these strains to be viable, they contained both an RFP-marked rescuing array for *pha-1* and a GFP-marked rescuing array for *sup-37*. Suppression of the *pha-1* deletions was ascertained by the presence of RFP<sup>-</sup>/GFP<sup>-</sup> larvae that arrest at the L1 stage because of the absence of rescuing *sup-37*<sup>+</sup> activity. In contrast, RFP<sup>-</sup>/GFP<sup>+</sup> progeny arrested as embryos with characteristic *pha-1* defects. Finally, *pha-1* deletion mutants harboring the *sup-37*(*e2215*) missense allele,

failed to segregate RFP<sup>-</sup> progeny that escaped past embryonic arrest, indicating that this allele failed to suppress the *pha-1* deletions.

#### **Intragenic complementation tests**

Complementation tests among the three deletion alleles of *sup-37* (*tm356*, *tm481*, and *tm1083*) were performed as follows. To generate *tm356*/*tm1083* trans-heterozygous animals, wild-type males were mated with *tm1083*/*dpy-11 unc-42* hermaphrodites, and F<sub>1</sub> cross-progeny males were subsequently mated to *tm356*/*dpy-11 unc-42* hermaphrodites. Eighty viable wild-type putative cross-progeny hermaphrodites were examined for the presence of both deletions by poison-primer PCR. If *tm356* and *tm1083* fail to complement, then none of the viable cross-progeny should be *tm356*/*tm1083*. If *tm356* and *tm1083* can complement one another, then one-seventh of the viable non-*Dpy Unc* cross-progeny hermaphrodites should be *tm356*/*tm1083*. Notably, of the 80 hermaphrodites analyzed, eight were verified to be cross-progeny that were heterozygous for *tm1083* but were balanced by the *dpy-11 unc-42* chromosome coming from the mother. If *tm356* and *tm1083* had complemented, we would have expected that on average four of the eight strains would carry the *tm356* deletion chromosome. In contrast, 24 additional verified cross-progeny contained a wild-type allele along with *tm356*.

Complementation tests of *tm481* with *tm356* (and *tm1083*) were performed as follows. Wild-type males were mated with hermaphrodites homozygous for *tm481*, and cross-progeny F<sub>1</sub> males were mated to *tm356*/*dpy-11 unc-42* hermaphrodites. Forty viable cross-progeny hermaphrodites from each cross were isolated, allowed to produce F<sub>2</sub>'s, and subsequently genotyped for the presence of deletions by poison-primer PCR. If *tm481* and *tm356* fail to complement, then *tm481*/*tm356* segregants (one-fourth of the total) would be nonviable and therefore absent from the adult population. Of the 40 viable cross-progeny analyzed, eight were *tm481*/*tm356* and gave rise to additional viable *tm481*/*tm356* animals, indicating that these deletion alleles do complement each other for viability. In the case of *tm1083*, 9/40 viable animals analyzed were *tm481*/*tm1083*, which in turn produced viable *tm481*/*tm1083* animals, indicating that these deletions also complement for viability.

To test for complementation of *sup-37*(*tm481*) and *sup-37*(*e2215*), *pha-1*(*e2123ts*) males were crossed with *tm481* hermaphrodites at 16°. Cross-progeny F<sub>1</sub> males of genotype *pha-1*(*e2123ts*)/+; *tm481*/+ were subsequently crossed with *pha-1*(*e2123ts*); *sup-37*(*e2215*) hermaphrodites at 25°. Twenty cross-progeny hermaphrodites were placed on individual plates, allowed to produce progeny, and then genotyped for both *pha-1*(*e2123ts*) and *tm481*. If *tm481*/*e2215* can suppress *pha-1*(*e2123ts*) lethality at 25°, one-fourth of the total cross-progeny should be of genotype *pha-1*(*e2123ts*); *tm481*/*e2215*. Whereas 12/20 cross-progeny animals tested were homozygous for *pha-1*(*e2123ts*), none

of the 12 animals were *tm481/e2215*, indicating that *tm481* and *e2215* complement for suppression. The above test was also repeated by mating *pha-1(e2123ts)/+*; *tm481/+* males into *pha-1(e2123ts) dpy-18; sup-37(e2216)* hermaphrodites at 25°. Twenty non-Dpy cross-progeny hermaphrodites were picked, allowed to produce F<sub>2</sub>'s, and then genotyped for *pha-1(e2123ts)* and *tm481*. Whereas 9/20 animals were *tm481/e2216*, none of the animals tested were homozygous for *pha-1(e2123ts)*, indicating a lack of suppression by *tm481/e2216*.

Lethal *sup-37* deletion alleles were also tested for their ability to suppress the lethal temperature-sensitive phenotype of the *pha-1(e2123ts)* at the nonpermissive temperature of 25°. As the protocol was very similar for alleles *tm356* and *tm1083*, only one case will be illustrated here. For the suppression analysis, *pha-1(e2123ts)* males were crossed with *tm356/dpy-11 unc-42* hermaphrodites. Cross-progeny males were then mated to *pha-1(e2123ts); sup-37(e2215)* hermaphrodites at 25°. Forty viable putative cross-progeny hermaphrodites were picked, allowed to lay embryos for ~8 hr at 25°, and then genotyped for *pha-1(e2123ts)* and *tm356*. The *e2123ts* mutation was monitored as described above, and the *tm356* deletion was assayed by poison-primer PCR. If *tm356* and *e2215* fail to complement for *pha-1* suppression, then one-eighth of the viable cross-progeny F<sub>1</sub>'s at 25° should be of the genotype *pha-1(e2123ts); e2215/tm356*. Of the 40 viable cross-progeny analyzed, 4 were *tm356/e2215* and also homozygous for *pha-1(e2123ts)*, indicating that *e2215* and *tm356* do not complement in the *pha-1* suppression assay. Similar findings were observed for *tm1083*; 4/40 viable animals analyzed were *tm1083/e2215* and homozygous for *pha-1(e2213ts)*. Furthermore, the viability of *tm356/e2215* and *tm1083/e2215* strains indicates that the *e2215* allele complements the lethality associated with the *tm356* and *tm1083* deletions. In separate experiments, *sup-37(e2216)* yielded similar results to those described above; *tm1083/e2216* and *tm356/e2216* animals were viable but failed to complement for suppression of *pha-1(e2123ts)* at 25°.

### RNAi

RNAi was carried out using strains from the Geneservice Library following standard feeding protocols (Ahringer 2005). To identify *sup-37*, ~90 RNAi clones corresponding to genes present within the SNP-mapped region were fed to strain GE24 [*pha-1(e2123ts)*] at 20° and 25° and scored for suppression of the *pha-1* temperature-sensitive lethal phenotype. A single positive RNAi construct corresponding to C01B7.1/ztf-12 was further confirmed by sequencing of the insert.

### qRT-PCR

Total RNA from the assayed strains was extracted from bleached embryos using Trizol reagent (Invitrogen). After DNAase I treatment, first-strand cDNA was synthesized using random primers and SuperScript II Reverse Transcrip-

tase (Invitrogen) at 42° for 1 hr. Using purified first strand cDNA, qRT-PCR was performed using the BioRad SYBR Green supermix in a BioRad iCycler with the following reaction conditions: initial denaturation at 95° for 3 min, followed by 40 cycles of denaturation at 95° for 30 sec, and a combined annealing and extension step at 60° for 30 sec. Fold change in the transcript levels was calculated using the ΔΔCt method. All the samples were analyzed in triplicate and data were tested for reproducibility using an independent biological repeat.

### Construction of plasmids

*sup-37* transcriptional GFP fusion constructs (*P<sub>sup-37</sub>::GFP*) pDF139/142 were prepared by inserting an ~3.0-kb promoter fragment amplified using the primer pairs 5'-AAACTGCAGCCTCACACATCATTCCACAT-3' and 5'-CGGGATCCGTCTAACTGGTCGGGAGAACATTGA-3' into the Fire vectors pPD95.77 and pPD95.69, respectively. The ~3.0-kb fragment includes the first 10 codons of exon 1 along with sequences upstream of C01B7.1 that extend to the adjacent upstream gene (C01B7.3). pPD95.69 differs from pPD95.77 in that the encoded GFP contains a nuclear localization signal. A *P<sub>sup-35</sub>::GFP* transcriptional fusion was constructed by inserting an ~730-bp genomic fragment consisting of the upstream *sup-35* promoter-enhancer region into pPD95.69 using the primer pairs 5'-GCTCTAGATGA TAGTCGTGTCGGTGGTCGTC-3' and 5'- CGGGATCCACGT GGGCACGCAAAGTGTGAGC -3'. All recombinant clones were verified by sequence analysis.

To create a SUP-37 translational reporter (*P<sub>sup-37</sub>::SUP-37::mCherry*), the genomic *sup-37* promoter region (1140-bp upstream sequence) was amplified using the following primers: 5'-AAAAAACTGCAGCATCTCGCTTCCGATCGCG-3' and 5'- CCCCCCTCTAGACAGGTGATCTGGAAAACATAGTTG-3'. This PCR product was cloned into *Pst*I and *Xba*I sites of plasmid L3691 (Fire Lab Vector kit) and verified by sequencing to generate plasmid pDF146. To create the cDNA clone containing the complete *sup-37* isoform A sequence, we first inserted 1003 bp from the *sup-37* cDNA clone YK817.g3 into the host plasmid containing *sup-37* clone YK1129.g7. Full-length *sup-37* cDNA was then PCR amplified from the resulting cDNA clone using the following primers: 5'-AAA AAAGGCGCGCCATGAGCATCAGCGGAGAGGACAAC-3' and 5'-CCCCCAGGTACCGGATCAGAAGAGACACCATCATCATC TTCTCCATC-3'. This product was cloned in frame with GFP into plasmid pDF146 using sites for *Ascl* and *KpnI*, thus placing the cDNA encoding SUP-37::GFP 24 nucleotides downstream from the inserted *sup-37* promoter. To create an mCherry version of the SUP-37 fusion reporter (pDF148), GFP sequences were excised from pDF147 using *KpnI* and *NheI* restriction enzymes and replaced with an mCherry sequence amplified from pJA304 using the following primers: 5'-AAAAAGGTACCGGGAGGTGGAGGTGGAGCTATGG TCTCA-3' and 5'- AAAAAGCTAGCTTACTTATAACAATTAT CCATGCCACCTGTCGAGTGCCG -3'. The mCherry amplicon also contained a 5'-spacer sequence encoding five glycines

and an alanine to facilitate folding and function of the fusion protein. The *sup-37* cDNA, GFP, and mCherry sequences were further verified by sequencing.

To generate the  $P_{myo-2}::SUP-37$  construct, *sup-37* cDNA was PCR amplified from the cDNA clone YK1129.g7 using the following primers: 5'-CCAAAGCTAGCATGAGCATTAGCGGAGAGGACAAC-3' and 5'-GGGCCTGGTACCTTAATCAGAGA GACACCATCATCTTCCATC-3'. This PCR amplicon was cloned into *Nhe*I and *Kpn*I sites of L2531 plasmid (Fire Lab Vector kit) and verified by sequencing.

#### Feeding assays and pharyngeal pumping

For bead internalization assays, NGM plates were seeded with a mixture of 20  $\mu$ l of fluorescent beads (Fluoresbrite 0.5- $\mu$ m Polychromatic Red Microspheres from Polysciences) in 1 ml of overnight cultures of **OP50**. The plates were incubated at 20°, and bead ingestion by L1 larvae was monitored by DIC/fluorescence microscopy. NGM plates seeded with **OP50** that expresses GFP (Labrousse *et al.* 2000) were prepared in a similar way as regular **OP50**-NGM plates, and fluorescence was monitored by DIC/fluorescence microscopy.

To assess pharyngeal pumping, WY733 adults (genotype *sup-37(tm356)V; fdEx174 [sup-37(+); pTG96(sur-5::gfp)]*) were allowed to lay eggs overnight under standard conditions. The next day, a glass cover was gently placed over the middle part of the bacterial lawn, followed by time-lapse microscopy of L1's with a  $\times 40$  objective, a Nikon Eclipse E600 microscope, a CoolSnap digital camera, and OpenLab software. Intervals of 30 sec were recorded at ambient temperature (~25°). Six *sup-37* mutant homozygotes were distinguished from two *sup-37*(+) siblings by the absence of the *fdEx174* array that expresses GFP and rescues *sup-37* (*tm356*). Pumping behavior and rates were determined following playback of the recordings at low speeds. Pumping was also grossly examined with a dissecting microscope capable of fluorescence and  $\times 110$  magnification.

#### Genetic mosaic analysis

Healthy L4 or young adult segregants from the WY733 strain were examined with a dissecting microscope equipped for fluorescence for mosaic patterns of nuclear green fluorescence (Yochem *et al.* 1998), conferred by **pTG96**, indicating mitotic nondisjunction of the *fdEx174* extrachromosomal array that also contains *sup-37*(+) DNA. The mosaics were then examined with a compound microscope, and the embryonic cell that must have lost the array during development of a particular mosaic animal was deduced from the anatomical pattern of fluorescence on the basis of the nearly invariant cell lineage of *C. elegans* (Sulston *et al.* 1983).

Although they can be more difficult to interpret, a small number of mutant mosaics were also analyzed. WY733 adults were removed from plates after laying eggs overnight, thereby producing progeny that had hatched within a narrow timeframe. Two days later, these plates, which contain a partially synchronous population of healthy worms, were examined for arrested L1's that also exhibited GFP,

indicating nonrescued mosaics that had nevertheless inherited the array. These plates also were a source of some of the healthy mosaics and allowed an assessment of whether or not certain classes of mosaics, although rescued for early requirements of *sup-37*, had other disadvantages in growth or development.

#### Microscopy of *pha-1* and *sup-37* expression

Fluorescence microscopy was performed using a Nikon Eclipse microscope. Quantification of the GFP and mCherry fluorescence in embryos was carried out using Open Lab software version 5.0.2. All images were captured using identical exposure times, and all embryos used in our analysis were of similar developmental stages (~200–300 cells). An average of the mean fluorescence was calculated to compare expression levels. *P*-values were determined using a two-tailed Student's *t*-test.

## Results

#### Molecular identification of *sup-37*

Recessive mutations in *sup-37* can suppress hypomorphic alleles of *pha-1* (Schnabel *et al.* 1991) as well as the synthetic lethal phenotypes of *lin-35*; *ubb-18*, *lin-35*; *pha-1*, *ubb-18*; *pha-1*, and *pha-1*; *ari-1*(RNAi) double mutants (Fay *et al.* 2004; Qiu and Fay 2006). To better understand the role of *sup-37* in pharyngeal development and genetic suppression, we molecularly identified the *sup-37* locus. We initially verified the location of *sup-37* on LGV (Schnabel *et al.* 1991) and then further refined the position of *sup-37* using genetic and SNP mapping methods. These approaches narrowed the *sup-37* locus to an ~300-kb region containing 95 predicted genes. To identify *sup-37*, 90 RNAi-feeding clones corresponding to this region were tested for suppression of *pha-1(e2123ts)* temperature-sensitive lethality at 20° and 25°. A single RNAi clone that targeted gene **C01B7.1/ztf-12** showed strong suppression of *pha-1(e2123ts)* at the nonpermissive temperature of 25° and also at the semipermissive temperature of 20°, suggesting that **C01B7.1** defines the *sup-37* locus (Figure 1; Table 1; data not shown). In addition, RNAi of **C01B7.1** suppressed the synthetic lethal phenotypes of *lin-35*; *ubb-18*, *lin-35*; *pha-1*, and *ari-1*; *pha-1* double mutants (Table 1), consistent with our previous observations.

To obtain further evidence that **C01B7.1** defines *sup-37*, we carried out transgenic rescue experiments (also see below). Extrachromosomal arrays containing wild-type copies of **C01B7.1** efficiently reverted the viability of *pha-1(e2123ts); sup-37(e2216)* mutants at 25°, such that animals containing GFP-marked **C01B7.1** arrays arrested as embryos or larvae and displayed pharyngeal morphogenesis defects characteristic of *pha-1(e2123ts)* single mutants (see *Materials and Methods*). Additionally, we sequenced the genomic region encompassing **C01B7.1** in six independently isolated alleles of *sup-37* (Schnabel *et al.* 1991). Three of the *sup-37* alleles (*e2214*, *e2215*, and *t1955*) showed an identical G-to-

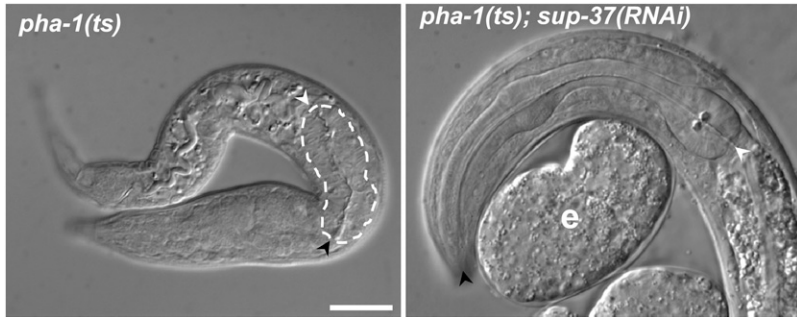


**Figure 1** Suppression of pharyngeal defects by *sup-37*. DIC images of *pha-1(e2123ts)* (left) and *pha-1(e2123ts); sup-37(RNAi)* (right) embryos at 25°. Black and white arrowheads indicate anterior and posterior pharyngeal boundaries, respectively. The abnormal pharynx in the *pha-1(e2123ts)* mutant is also outlined. e, embryo. Bar for both left and right, 10  $\mu$ m.

A transition in exon 3, leading to a change from aspartic acid to asparagine at amino acid (aa) position 479 (Figure 2; Table 2; Supporting Information, Figure S1). Two other alleles of *sup-37* (*e2216* and *t1070*) contained an identical C-to-T transition in exon 3, leading to a change from serine to leucine at aa position 481 (Figure 2; Table 2; Figure S1). The final allele of *sup-37* (*t1954*) contained a G-to-A transition in exon 3 leading to a substitution of a serine for glutamate at aa position 462 (Figure 2; Table 2; Figure S1). These results, together with findings from transgenic rescue and RNAi phenocopy studies, demonstrate that *sup-37* corresponds to *C01B7.1/ztf-12*.

#### *sup-37 encodes a predicted Zn-finger protein*

WormBase predicts three different isoforms of *C01B7.1* (a–c). The two long isoforms (*C01B7.1a* and *C01B7.1c*) contain eight exons, which differ only in their fourth exon (Figure 2; Figure S2). The shorter isoform (*C01B7.1b*) is composed of only four exons; these correspond to the first four exons of the *C01B7.1c* isoform, but the *C01B7.1b* isoform also includes additional 3' sequences (Figure 2; Figure S2). To confirm these predictions, we sequenced available EST clones (NBP Japan) corresponding to the *C01B7.1* locus. Sequencing validated the existence of isoforms a–c and identified an additional long isoform (*C01B7.1d*; clone *yk817g03*) that is most similar to *C01B7.1c* but is missing the fifth exon, which is common to *C01B7.1a* and *C01B7.1c* (Figure 2; Figure S2). These predictions are further supported by available RNA sequencing data (WormBase) and by homology comparisons with other nematode species (Figure S3).

InterProScan predicts seven C2H2-like Zn-finger motifs at aa positions 93–116, 122–145, 413–434, 444–469, 592–615, 795–815, and 822–845 in isoforms *C01B7.1a* and *C01B7.1c*; the *C01B7.1d* isoform contains the same Zn fingers with the three C-terminal fingers located at aa positions 570–593, 773–793, and 800–823. The *C01B7.1b* isoform contains only the first four Zn fingers in common with the other isoforms. Whereas Zn fingers 1, 3, and 6 are 100% conserved in putative orthologs of *ztf-12* in *C. remanei* and *C. briggsae*, the other Zn fingers show slight variations (Figure S3). All the identified *sup-37* missense mutations are contained within the common fourth exon of all the *sup-37* isoforms and occur either within or just downstream of the fourth Zn finger (Figure 2; Figure S1).

In addition, the identified missense mutations alter aa residues that are completely conserved in *SUP-37* homologs from *C. remanei* and *C. briggsae* (Figure S3).

#### *sup-37 is an essential gene*

In addition to the point mutations described above, sequence analysis confirmed three *sup-37* deletion alleles generated by the Japanese knockout consortium. *tm1083* is an in-frame insertion–deletion mutation that removes 237 aa of *SUP-37* from positions 87–323 and inserts a single aa at position 87 (Figure 2; Figure S2). *tm356* is a 576-bp deletion leading to a frameshift and premature stop codon following position 501 (Figure 2; Figure S2). Both *tm1083* and *tm356* are predicted to affect all isoforms of *sup-37* and are likely to comprise molecular nulls (Figure 2). The region deleted in *tm1083* removes the first two Zn fingers, whereas the regions deleted by *tm356* do not affect any of the Zn fingers. Interestingly, *tm356* and *tm1083* homozygous mutants are not viable and undergo early larval arrest, indicating that *sup-37* is an essential gene (also see below). Consistent with this, transgenic arrays expressing wild-type *sup-37* are sufficient to fully rescue the lethality of *tm356* and *tm1083* homozygous mutants. *tm481* is a 509-bp deletion that affects only the b–d isoforms of *sup-37* and does not affect the N-terminal Zn fingers (Figure 2). In contrast to *tm1083* and *tm356*, *tm481* homozygous mutants are viable, indicating that *sup-37* splice variants containing the exon deleted by *tm481* (*C01B7.1b–d*) do not perform essential functions (Table 2).

**Table 1** Suppression of pharyngeal defects by *sup-37*

Genotype	Fertile adults (%)
<i>pha-1(e2123ts)</i> (16°)	96.7 (n = 365)
<i>pha-1(e2123ts)</i> (25°)	0 (n = 404)
<i>pha-1(e2123ts); vector RNAi</i> (25°)	0 (n = 340)
<i>pha-1(e2123ts); C01B7.1 RNAi</i> (25°)	98.4 (n = 312)
<i>lin-35; ubc-18</i> (20°)	0 (n = 137)
<i>lin-35; ubc-18; vector RNAi</i> (20°)	2.4 (n = 187)
<i>lin-35; ubc-18; C01B7.1 RNAi</i> (20°)	66.4 (n = 164)
<i>lin-35; pha-1(fd1)</i> (20°)	0 (n = 248)
<i>lin-35; pha-1(fd1); vector RNAi</i> (20°)	3.1 (n = 143)
<i>lin-35; pha-1(fd1); C01B7.1 RNAi</i> (20°)	74.6 (n = 151)
<i>ari-1(tm2549); pha-1(e2123)</i> (16°)	1.5 (n = 338)
<i>ari-1(tm2549); pha-1(e2123); vector RNAi</i> (16°)	1.7 (n = 192)
<i>ari-1(tm2549); pha-1(e2123); C01B7.1 RNAi</i> (16°)	70.2 (n = 214)

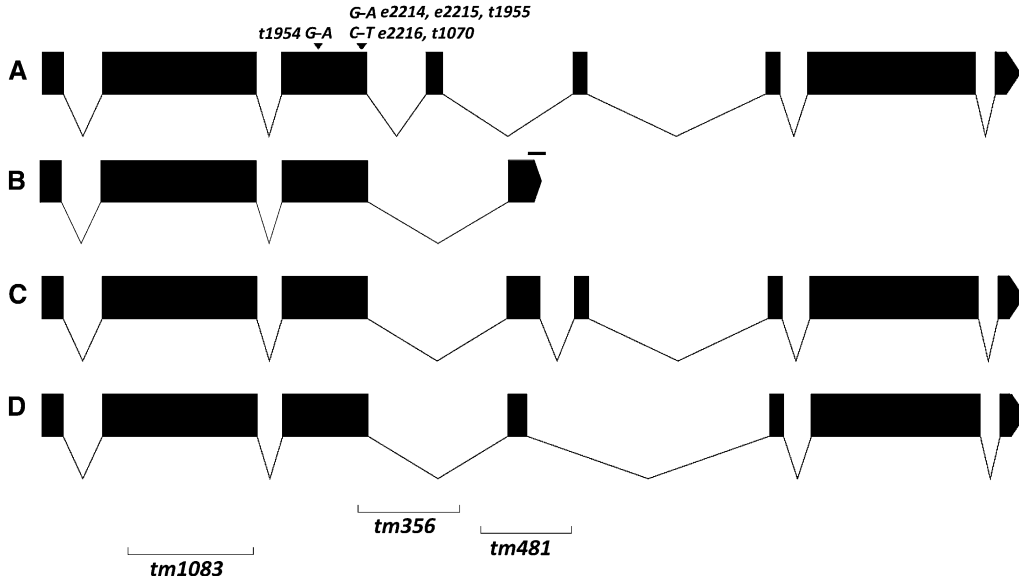


**Figure 2** Schematic depiction of the *sup-37* locus. Locations of exons, point mutations, and deletions are indicated. Note four distinct isoforms (A–D).

### Functional analysis of *sup-37* alleles

To characterize the activities of the identified *sup-37* alleles, we carried out genetic complementation tests (Table 3; also see *Materials and Methods*). In contrast to all other combinations assayed, *tm356/tm1083* *trans*-heterozygous mutants were not viable, further demonstrating that *sup-37* is an essential gene. Combinations of the *tm356* or *tm1083* deletion with *sup-37* missense alleles were uniformly viable. This result, together with *sup-37(RNAi)* findings (Figure 1; Table 1), indicates that the *sup-37* missense alleles are hypomorphic. In addition, *pha-1(e2123ts)* mutants that were *trans*-heterozygous for either of the two null *sup-37* deletions (*tm356* or *tm1083*) and two of the tested missense alleles (*e2215* and *e2216*) were fully suppressed at 25° (Table 3). In contrast, *tm481* homozygous mutants did not suppress *pha-1(e2123ts)* mutants, and *tm481* complemented all other tested *sup-37* alleles in both viability and *pha-1* suppression assays. Thus, isoforms containing the exon deleted by *tm481* (b–d) do not appear to have appreciable roles in either viability or pharyngeal morphogenesis.

We further note that growth of homozygous *tm481* mutants at 25° leads to a high incidence of sterility and that these sterile animals are defective at oogenesis (data not shown). However, several pieces of evidence indicate that

this temperature-sensitive sterility may not result specifically from a reduction in *sup-37* activity. (1) The sterile phenotype of *tm481* is complemented in *trans* by both *tm356* and *tm1083* null deletion mutations (Table 3). (2) *tm481* sterility is not rescued by *sup-37(+)*-containing extrachromosomal arrays that rescue other *sup-37*-associated phenotypes (data not shown). (3) *sup-37(RNAi)* at 25° does not result in high levels of sterility in N2 animals (data not shown). Thus, the sterility associated with *tm481* may be due to a closely linked mutation that was not separated from the *sup-37* locus following outcrossing.

### *SUP-37* is required for normal pharyngeal pumping

The *sup-37* null deletion alleles *tm356* and *tm1083* exhibited a fully penetrant L1 larval arrest when homozygous. Furthermore, homozygous *tm356* and *tm1083* mutants displayed no morphological abnormalities indicative of developmental defects. Also, the mutants can move normally and exhibit foraging behavior. These observations, together with our observation that *sup-37* is expressed strongly in the larval pharynx (see below), suggested that *sup-37* null mutants may have defective pharynges that preclude proper feeding. Consistent with a feeding defect, the intestines of the mutants have refractile vacuoles indicative of starvation (Schroeder *et al.* 2007). To test this, homozygous *tm356* and

**Table 2** Summary of *sup-37* alleles

<i>sup-37</i> allele	Mutation class	Isoforms affected <sup>a</sup>	Phenotype	<i>pha-1</i> suppression <sup>b</sup>
<i>tm356</i>	Deletion	a, b, c, d	Larval arrest	Yes
<i>tm481</i>	Deletion	b, c, d	Viable	No
<i>tm1083</i>	Insertion/deletion	a, b, c, d	Larval arrest	Yes
<i>e2214</i> ( <i>e2215, t1955</i> )	Missense	a, b, c, d	Viable	Yes
<i>e2216</i> ( <i>t1070</i> )	Missense	a, b, c, d	Viable	Yes
<i>t1954</i>	Missense	a, b, c, d	Viable	Yes

<sup>a</sup> See Figure 2.

<sup>b</sup> Suppression of the Pun phenotype of *pha-1(e2123ts)* at 25°.

**Table 3** Summary of *sup-37* complementation analysis

	<i>tm356</i>	<i>tm481</i>	<i>tm1083</i>	<i>e2215</i>	<i>e2216</i>
<i>tm356</i>	Let	V	Let	V,S	V,S
<i>tm481</i>	V	V, NS	V	V, NS	V,NS
<i>tm1083</i>	Let	V	Let	V,S	V,S

Let, lethal; V, viable; S, suppression; NS, no suppression. Suppression was scored in a *pha-1(e2123ts)* homozygous background at 25°. Note that suppression was not scored for all possible genotype combinations. In the case of *tm356/tm481* and *tm1083/tm481* 34/50 and 18/25 hermaphrodites were fertile at 25°, respectively.

*tm1083* mutants were fed fluorescent *Escherichia coli* (OP50) and analyzed by compound microscopy. In contrast to wild-type L1 larvae, which uniformly contained intact fluorescent OP50 from the anterior pharyngeal lumen up to the posterior pharyngeal bulb ( $n = 75$ ), 100% ( $n = 75$ ) of *sup-37* null mutants contained fluorescent OP50 up to the anterior bulb only (Figure 3, A–D). In addition, 100% ( $n = 75$ ) of *tm356* and *tm1083* homozygous mutants failed to internalize fluorescent beads past the grinder, whereas wild-type animals uniformly contained beads throughout the entire pharyngeal–intestinal tract (Figure 3, E–H and data not shown;  $n = 75$ ).

To understand the feeding defect in more detail, pharyngeal pumping of six *sup-37(tm356)* homozygotes was compared with that of two nonmutants by time-lapse video microscopy. The rate of pumping for the two nonmutants was 195 and 192 pumps per minute, both of which are similar to the wild-type rate of 240 pumps per minute at room temperature (Altun *et al.* 2002–2010). In contrast, five of the six mutants, when they did pump, exhibited the much lower rates of 36, 58, 53, 60, and 30 pumps per minute. The sixth mutant failed to pump all together. Moreover, pumping by the mutants was invariably less robust than that of the wild-type animals: contractions of the corpus, the anterior half of the pharynx, were not seen, and the contractions of the terminal bulb appeared weak and sometimes sporadic. The contractions of the terminal bulb, although insufficient for thriving, may nevertheless be sufficient for the ingestion of the small amounts of fluorescent bacteria and beads present in the mutants (Figure 3).

#### The focus of *sup-37* activity for proper feeding may be the pharynx

As noted above, *sup-37* homozygous null mutants are starved and invariably arrest growth and development in the first larval stage. Their impaired pharyngeal pumping implies a defect in the function of pharyngeal muscle cells, as pharyngeal neurons are largely dispensable for pumping (Avery and Horvitz 1989). To investigate this notion in more detail, healthy genetic mosaics that segregated from WY733 were analyzed. Because these mosaics were healthy and had reached the L4 or young adult stage, it is reasonable to assume that wild-type *sup-37* present on the *fdEx174* array functioned in these mosaics in the proper part of the cell lineage required for normal pharyngeal pumping.

The only early cells of the lineage that did not undergo losses of the array were P<sub>1</sub>; EMS, one of the daughters of P<sub>1</sub>; and MS, a granddaughter of P<sub>1</sub>, indicating that the focus of

gene activity descends from MS. A few mutant mosaic—GFP (+) L1s that were arrested with a starved appearance were also examined, although caution is required in interpreting them, as developmental arrest could result from effects other than a lack of wild-type *sup-37* gene activity. They could, for example, have been sick for unknown reasons—perhaps from overexpression of the array in certain parts of the cell lineage, following the increase in copy number that results from nondisjunction. Nevertheless, there were seven arrested mosaics that could be easily characterized. Two had a loss in P<sub>1</sub>, three had a loss in EMS, and two had a loss in MS. Another arrested L1 had suffered losses of the array in ABa, MS, and P<sub>2</sub>. These mosaics are therefore the reciprocal of the healthy mosaics, none of which had a loss in P<sub>1</sub>, EMS, or MS (Figure 4). Other mosaics that were arrested as starved L1's had more limited inheritance of the array.

Both approaches implicated one or more descendants of MS as the focus of *sup-37* gene activity. A paradox, however, was the isolation of one MSa and three MSp losses. That is, MSa can compensate for a loss in its sister, MSp, and vice versa. An interpretation of this variability is that the focus of gene activity is composed of redundant cells, some of which descend from MSa and some from MSp. Another interpretation is that the focus is multinucleated, with some nuclei in the syncytium descending from MSa and some from MSp. Inheritance of *sup-37*(+) from either progenitor would then be sufficient for rescue.

Although a single cellular focus could not be pinpointed, the mutant phenotype, the mosaic analysis, and the structure of the pharynx together raise the possibility that the focus is a gestalt composed of the three pm3 and the three pm4 muscles of the pharynx. These muscles are responsible for contraction of the corpus (Altun *et al.* 2002–2010), a contraction not seen in *sup-37(tm356)* homozygotes. The pm1 and pm2 muscles are also involved in contraction of the corpus, but these descend solely from ABa and therefore cannot be critical foci of *sup-37*. One reason for the inability to pinpoint the focus might be the lineal complexity of these muscles, because each of them is dinucleate, as follows: pm3 dorsal, one nucleus from MSa and the other from MSp; pm3 left subventral, both nuclei from ABa; pm3 right subventral, both nuclei from ABa; pm4 dorsal, one nucleus from MSa and the other from MSp; pm4 left subventral, both nuclei from MSa; pm4 right subventral, one nucleus from ABa, the other from MSp (Albertson and Thomson 1976; Sulston *et al.* 1983). An MSp loss would therefore leave all six muscles *sup-37*(+). An MSa loss would render the pm4 left subventral muscle genotypically *sup-37*(−), but the remaining five muscles would be *sup-37*(+), which might be sufficient for pumping. The ABa(+) MS(−) mosaics are problematic, because the pm4 right subventral muscle, which has a nucleus that descends from ABa, should be positive for the array. Perhaps one positive muscle is not sufficient for adequate contraction of the metacorpus, which is mediated by the pm4 muscles. In an ABa(−) MS(+) mosaic, all three pm4 muscles are plus, but only one pm3

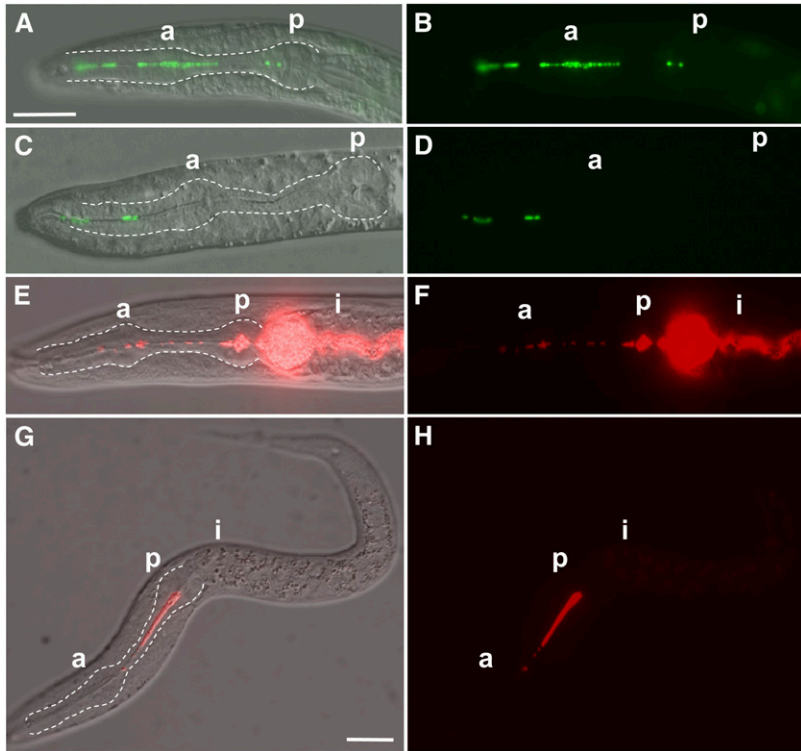


**Figure 3** Bacteria and fluorescent bead ingestion by wild type and *sup-37* mutants. GFP-expressing OP50 *Escherichia coli* were fed to wild-type N2 (A and B) and *sup-37* (*tm356*) mutants (C and D). (A and C) GFP-DIC overlays. a, anterior; p, posterior pharyngeal bulbs, respectively. Note that bacteria are present within the pharyngeal lumen of N2 animals from the anterior buccal cavity to the posterior bulb, where they are mechanically processed leading to loss of fluorescence in more posterior portions of the pharynx and intestinal tract (A and B). In contrast, *sup-37* mutants are unable to ingest bacteria beyond the anterior bulb (C and D). Fluorescent bead ingestion in wild type (E and F) and *sup-37*(*tm356*) mutants (G and H). E and G show fluorescent-DIC overlays. i, intestine. N2 animals contain beads in the lumen of the pharynx and throughout the intestine (E and F), whereas *sup-37* mutants do not contain beads past the posterior bulb (G and H). Bars, 10  $\mu$ m in A (A–F); 10  $\mu$ m in G (G and H).

muscle is plus. Perhaps the pm4 muscles of the metacorpus provide most of the contractile force of the corpus.

Several of the arrested mutant mosaics provided evidence in support of this interpretation of the focus and raised the possibility that robust contraction of the corpus requires that both the pm3 muscles and the pm4 muscles be functional. In six of the mutant mosaics, all three of the pm4 muscles were minus for the *sup-37*(+) array, but some or all of the pm3 muscles were plus. Conversely, all three of the pm3 muscles were minus and all three of the pm4 muscles plus in two of the mutant mosaics. Thus, the specific requirement for *sup-37* in the pharynx is apparently somewhat flexible,

but is required within one of at least several combinations of pm3 and pm4 muscle cells. We also note that we attempted to rescue the pumping defect of *sup-37* null mutants using a P<sub>myo-2</sub>::SUP-37 reporter, which should express SUP-37 specifically in pharyngeal muscles. This construct, however, proved to be highly toxic, suggesting that overexpression of SUP-37 may be deleterious to pharyngeal muscle function or development.

#### The mosaic analysis indicates other functions for *sup-37*

E(-) mosaics, those lacking the *sup-37*(+) array in all cells of the intestine, were easy to identify (Figure 4). These mosaics

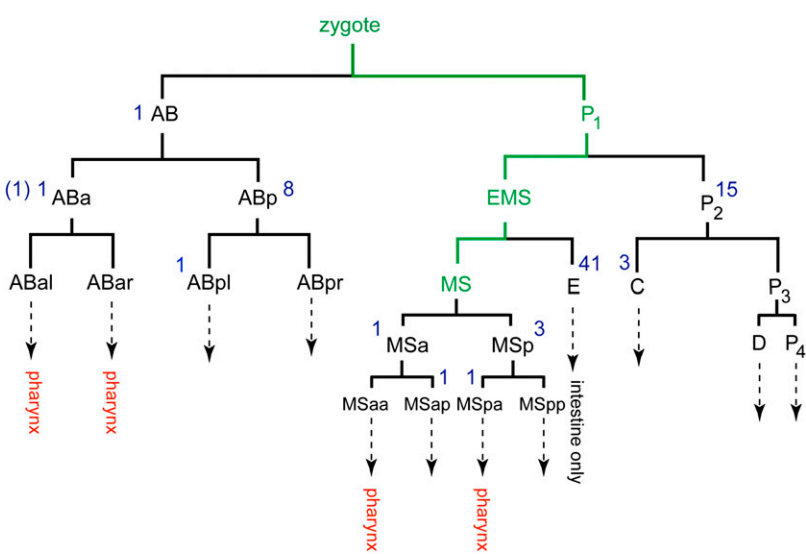


**Figure 4** Summary of the mitotic losses in healthy *sup-37* (*tm356*) genetic mosaics. On the basis of anatomical studies, the number of healthy animals that had negative clones—likely a consequence of nondisjunction—is shown next to the early embryonic cell that failed to inherit the *sup-37*(+) *sur-5::GFP* array (*fdEx174*) following mitotic division. One of the ABa losses is shown in parentheses, because the animal, although rescued for the *sup-37* feeding defect, was not as healthy as the other animals that had had an AB or ABa loss. Those cells that contribute descendants to the pharynx or to the intestine are shown. Blastomeres that did not give rise to negative clones are shown in green, as is their lineal relationship.

were invariably slightly retarded in growth relative to non-mosaics on partially synchronous plates (L4s vs. adults). One half of them had a scrawny appearance; the remaining resembled normal worms. Thus, there may be a non-essential requirement for *sup-37* in the intestine, but this possibility has not been examined in detail. In addition, there appears to be a requirement for *sup-37* in the somatic gonad for proper ovulation, depending on which gonadal arm is plus or minus for the array. When an arm was negative for *sup-37*, the oocytes of that arm were abnormally small and were not in single file (Figure 5, C and D). Positive arms, on the other hand, have oocytes of normal appearance (Figure 5, A and B). The defect in the mutant arm appears to result from abnormally slow movement of oocytes into the spermatheca, a process that normally requires dilation of the distal part of the spermatheca and contractions of proximal sheath cells (Altun *et al.* 2002–2010; Greenstein 2005). In addition, on the basis of gross nuclear morphology, these oocytes appear to be endomitotic. The *sup-37* gene is not absolutely required for this process, as some oocytes can transit the spermatheca, and mosaics completely minus for the somatic gonad produce some progeny, which often exit the vulva as hatchlings. Whether the focus of gene activity is the spermatheca, the sheath cells, or both is not known.

#### Expression of *sup-37*

To determine the expression pattern of *sup-37* during development, we first generated extrachromosomal arrays expressing  $P_{sup-37}::GFP$  promoter fusions containing ~3.0 kb of *sup-37* upstream sequences. In addition, we made use of a strain containing an integrated  $P_{sup-37}::his-24::mCherry$  reporter containing ~1 kb of *sup-37* upstream sequences (Liu *et al.* 2009). All tested strains showed strong enrichment of reporter expression within the pharynx beginning at the ~500-cell stage of embryogenesis and continuing throughout larval development and adulthood (Figure 6, A–H). In addition, weak-to-modest levels of *sup-37* reporter expression were observed in all other cell types (Figure 6; data not shown). Expression of *sup-37* reporters in pharyngeal muscle is consistent with an autonomous role for SUP-37 in pharyngeal pumping. In addition, *sup-37* is temporally and spatially coexpressed with both *sup-35* and *pha-1* and shows a similar degree of enrichment in the pharynx as was observed for SUP-35::GFP (Fay *et al.* 2004; Mani and Fay 2009).

We also examined expression of full-length (isoform-a) SUP-37::GFP and SUP-37::mCherry fusion proteins. Both reporters localize predominantly to nuclei during late stages of embryogenesis (Figure 7, A and B; data not shown), consistent with a role for SUP-37 in the nucleus. Expression of these constructs was, however, relatively dim and quite variable as compared with the *sup-37* transcriptional reporters. Expression of the SUP-37 translational reporters was also occasionally detected in both the cytoplasm and nuclei of early-stage embryos at time points preceding morphogenesis (data not shown). In larval and adult stages, SUP-37::mCherry was expressed in the pharyngeal muscle groups

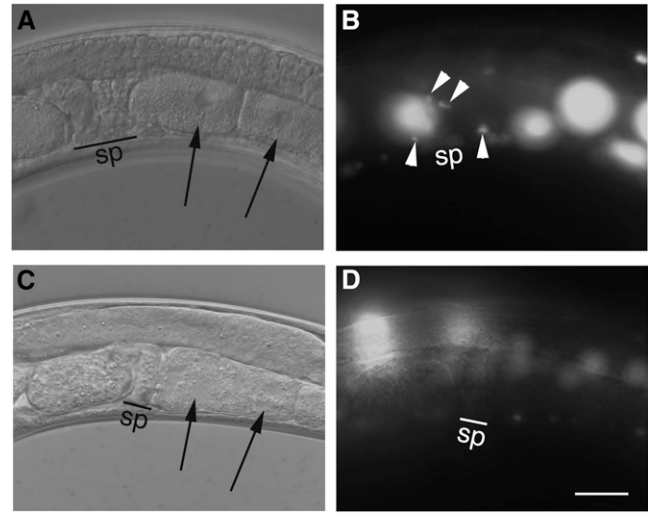


**Figure 5** Abnormal oocytes in a *sup-37(tm356)* somatic gonad mosaic. Adult hermaphrodite containing one *sup-37*(+) (A and B) and one *sup-37*(-) (C and D) somatic gonad arm. Arrows indicate oocytes. Lines indicate boundary of the spermatheca (sp). (A) Oocytes of reasonably normal appearance await entry into the spermatheca in single file (DIC optics). (B) Fluorescent image of the arm indicating expression of SUR-5::GFP from the *sup-37*(+) array (*fdEx174*) in nuclei (arrowheads) of the spermatheca. (C) DIC image of abnormal oocytes (arrows) in the *sup-37*(-) arm of the same animal. (D) Fluorescent image of this arm demonstrating a lack of SUR-5::GFP in nuclei of the spermatheca, one of several indications that the arm lacked *sup-37*(+) activity. Bar in D, 25  $\mu$ m in A–D.

pm3, pm4, and pm6, but not consistently in other cells of the pharynx (Figure 7, C and D). This result is strikingly consistent with our mosaic analysis indicating an essential function for SUP-37 in a subset of the pm3 and pm4 muscle groups. In addition, SUP-37::mCherry expression was faint but detectable in the spermatheca of adult hermaphrodites (data not shown). This observation is consistent with findings from the mosaic analysis demonstrating a requirement for *sup-37* in the somatic gonad to promote ovulation. Expression of SUP-37::mCherry was not detected in the somatic gonad sheath cells, which also play a role in ovulation. Although this might suggest a specific role for *sup-37* in the spermatheca, we observed several cases where at least some cells within the spermatheca of *sup-37(tm1083)* mutants were positive for SUP-37::mCherry expression, but these gonads were nevertheless defective at ovulation. Thus, SUP-37 might be required in sheath cells but is expressed at levels below our limits of detection. Alternatively, failure of SUP-37::mCherry to consistently rescue ovulation defects could be due to mosaicism of array within the spermathecal cells of affected animals or may be due to reduced activity of the fusion protein.

At present, it is unclear why the SUP-37 translational fusion reporters, which contain the same upstream regulatory sequences as that of the transcriptional reporters, differ from the transcriptional reporters in their pattern and intensity of expression. It is possible that the fusion proteins are unstable or targeted for degradation or that additional

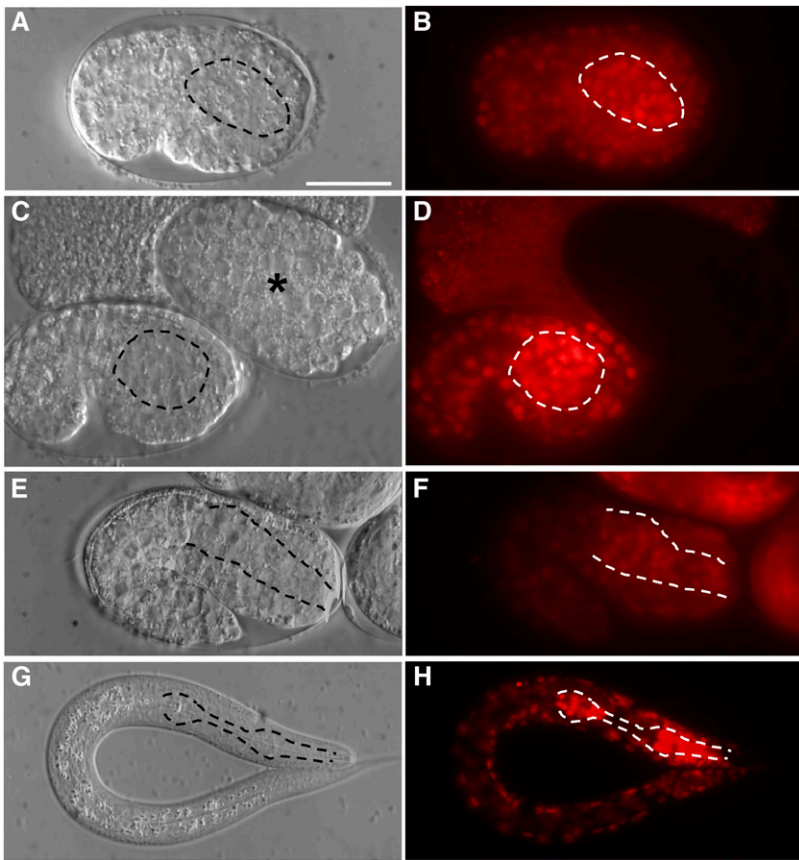


**Figure 6** *sup-37* transcriptional reporter expression. Transgenic animals carrying a *his-24::mCherry* reporter under the control of the *sup-37* promoter show broad expression in embryos, larvae, and adults. A, C, E, and G are corresponding DIC images of B, D, F, and H. Initial *P<sub>sup-37</sub>::his-24::mCherry* expression was coincident with the onset of morphogenesis and was consistently enriched in pharyngeal cells (A–H). Premorphogenetic ~200-cell-stage embryo (\*) in C and D shows no expression. Bar in A, 10  $\mu$ m in A–F; 50  $\mu$ m in G and H.

regulatory elements exist within the coding sequence of *sup-37*. In tests for biological activity, SUP-37::mCherry was found to rescue the embryonic lethality of *sup-37* (*tm1083*) null mutants, indicating that the fusion protein is biologically active. In summary, clear nuclear expression of the translational reporters is consistent with a role for SUP-37 in transcriptional regulation and places SUP-37 in the same cellular compartment as SUP-35 during latter stages of embryogenesis.

#### ***SUP-37 expression is not regulated by the LIN-35 or UBC-18-ARI-1 pathways***

We sought to determine whether *sup-37* expression is regulated by the LIN-35 or UBC-18-ARI-1 networks as was observed for *sup-35* (Mani and Fay 2009). In contrast to *P<sub>sup-35</sub>::GFP*, *P<sub>sup-37</sub>::GFP* expression did not change significantly in *lin-35(RNAi)*-treated embryos (Figure 8, G and H). We also did not detect a consistent increase in endogenous *sup-37* mRNA levels in *lin-35(n745)* mutants using qRT-PCR (Figure 8A). *sup-35* is positively regulated by HCF-1, which antagonizes LIN-35 activity and functions as a putative positive regulator of E2F target-gene transcription (Mani and Fay 2009). Whereas embryos containing *P<sub>sup-35</sub>::GFP* showed a significant decrease in GFP expression following *hcf-1(RNAi)*, embryos containing a *P<sub>sup-37</sub>::GFP* were unaffected by this treatment (Figure 8, C–H). Furthermore, *sup-37* mRNA levels, as well as *P<sub>sup-37</sub>::GFP* and *P<sub>sup-37</sub>::his-24::mCherry*

reporters, were not sensitive to inhibition of *ubc-18* or *ari-1* activity, indicating that UBC-18-ARI-1 does not regulate *sup-37* at the level of transcription (Figure 8, A and G; data not shown). Finally, in contrast to SUP-35::GFP, a SUP-37::mCherry fusion reporter was not affected by RNAi of either *ubc-18* or *ari-1*, indicating that UBC-18-ARI-1 does not regulate *sup-37* at the level of protein stability (Figure 8, I and J). Taken together, these results indicate that, unlike SUP-35, SUP-37 expression is not regulated by either the LIN-35 or UBC-18-ARI-1 pathways.

#### ***SUP-37 and SUP-35 may act in a common step to repress PHA-1 expression***

We previously reported that SUP-35 can inhibit the expression of *pha-1*, thereby providing an explanation for the suppression of hypomorphic alleles of *pha-1* by *sup-35* mutations (Mani and Fay 2009). Consistent with this, we found that mutations in *sup-37* led to a significant increase in the abundance of *pha-1* mRNA on the basis of both transcriptional and translational *pha-1* GFP reporters, although these effects were somewhat weaker than those observed for *sup-35* (Figure 9) (Mani and Fay 2009). The observed increase in *P<sub>pha-1</sub>::GFP* fluorescence in *sup-37* mutant embryos indicates that repression of *pha-1* by SUP-35 and SUP-37 occurs at the level of transcription (Figure 9, A–C and G) (Mani and Fay 2009). In addition, *sup-37(RNAi)* embryos had slightly increased levels of a functional PHA-1::GFP

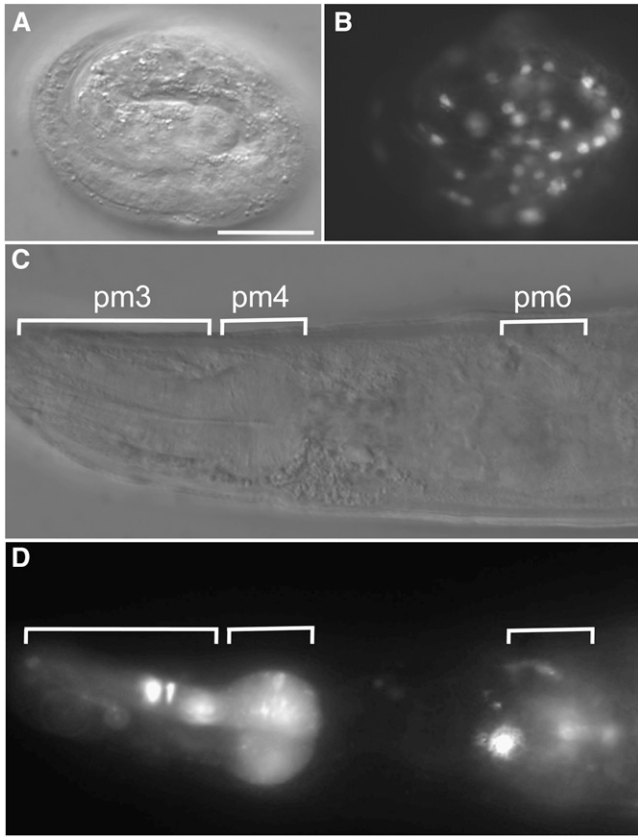


**Figure 7** SUP-37 translational reporter expression. A full-length isoform of SUP-37::mCherry reporter shows expression in embryos and adult tissues. A and C are corresponding DIC images of B and D. Late-stage embryos of strain WY803 (A and B) show localization of SUP-37::mCherry in nuclei of multiple cell types. Expression in the adult pharynx of strain WY835 (C and D) show expression of SUP-37::mCherry in the multinucleate muscle groups pm3, pm4, and pm6. In contrast to the embryo, expression in the adult pharynx is both nuclear and cytoplasmic. For images C and D, anterior is left. Bar in A, 10  $\mu$ m in A and B; 25  $\mu$ m in C and D.

translational fusion, suggesting that the increase in *pha-1* mRNA levels in *sup-37* mutants leads to a corresponding increase in PHA-1 protein levels (Figure 9, D–F and H).

As previously described, SUP-35 overexpression leads to embryonic and larval arrest that phenocopies *pha-1* LOF mutations (Mani and Fay 2009). Furthermore, arrest induced by SUP-35 overexpression is completely dependent on the presence of wild-type SUP-37, suggesting that SUP-37 may act downstream of SUP-35 to mediate *pha-1* transcriptional repression. Alternatively, SUP-37 could serve as an upstream activator of SUP-35 or may act in a pathway that is parallel to SUP-35. Finally, SUP-37 could act at the same level as SUP-35, possibly within a single complex. Several findings indicate that SUP-35 and SUP-37 may act at a common step. First, *sup-35*; *sup-37* double mutants did not show enhanced expression of *pha-1* relative to single mutants, suggesting that SUP-35 and SUP-37 are unlikely to act in either parallel or partially redundant pathways (Figure 8G). Second, *sup-37* mRNA levels were unaffected

by *sup-35* mutations, indicating that *sup-37* is not a downstream transcriptional target of SUP-35 (Figure 8A). Consistent with this, expression of a full-length SUP-37::mCherry fusion protein was not affected following *sup-35*(RNAi) (data not shown). Finally, SUP-35 mRNA levels were not affected by loss of *sup-37*, indicating that *sup-35* is not a transcriptional target of SUP-37 (Figure 8B). Our collective data suggest that SUP-37 and SUP-35 may act at the same step within a single pathway or complex to regulate PHA-1 expression and pharyngeal development.

#### Negative regulation of PHA-1 expression is not the primary mechanism of *pha-1* suppression by *sup-35* and *sup-37* mutations

Studies using a large chromosomal deficiency, *tDf2*, which deletes both *sup-35* and *pha-1*, as well as ~46–72 additional genes, suggested that loss of *sup-35* function could not suppress a complete loss of *pha-1* activity (Schnabel *et al.* 1991; Mani and Fay 2009). We sought to confirm these results using two deletion alleles of *pha-1*, *tm3671* and *tm3569*, which have been extensively backcrossed and can be maintained as homozygous stocks through the use of a *pha-1*-rescuing RFP-marked extrachromosomal array. Both *pha-1* deletion strains exhibit 100% lethality of self-progeny that fail to inherit the rescuing array, and these lethal embryos resemble *pha-1(e2123ts)* mutants at 25°. *pha-1(tm3671)* contains a 203-bp deletion that removes part of the second exon of *pha-1* and creates a premature stop codon, whereas *pha-1(tm3569)* contains an in-frame 568-bp deletion from exons 2–4, removing 149 amino acids of PHA-1. On the basis of the nature of these lesions as well as the phenotype of the mutant embryos, both deletions are presumed to be null alleles.

A summary of our findings on the suppression of the *pha-1* deletions can be found in Table 4. Surprisingly, we observed that *sup-35*(RNAi) can suppress the lethality of both *pha-1(tm3569)* and *pha-1(tm3671)*, such that both deletion mutations could be propagated as homozygotes when grown continuously on *sup-35*(RNAi); subsequent removal to control RNAi plates led to lethality of the *pha-1* deletion strains within two generations. Furthermore, *pha-1* deletion strains placed on *pha-1*(RNAi) *sup-35*(RNAi) double-RNAi plates were also suppressed, indicating that any residual activity of the *pha-1* deletions was unlikely to account for the ability of *sup-35*(RNAi) to achieve suppression. To determine whether *sup-37* mutations could also suppress *pha-1* null mutants, we tested one missense allele (*e2215*) and the two larval-lethal deletion alleles (*tm356* and *tm1083*) of *sup-37*. In the case of the *sup-37* deletions, additional methods were used to maintain strains carrying two separate lethal mutations (see *Materials and Methods*). Whereas the hypomorphic *sup-37(e2215)* allele failed to suppress *pha-1* null embryonic lethality, both null alleles of *sup-37* suppressed the embryonic lethality and morphogenesis defects of the *pha-1* deletions. In this case, suppressed animals arrested as wild-type-looking L1 larvae due to the

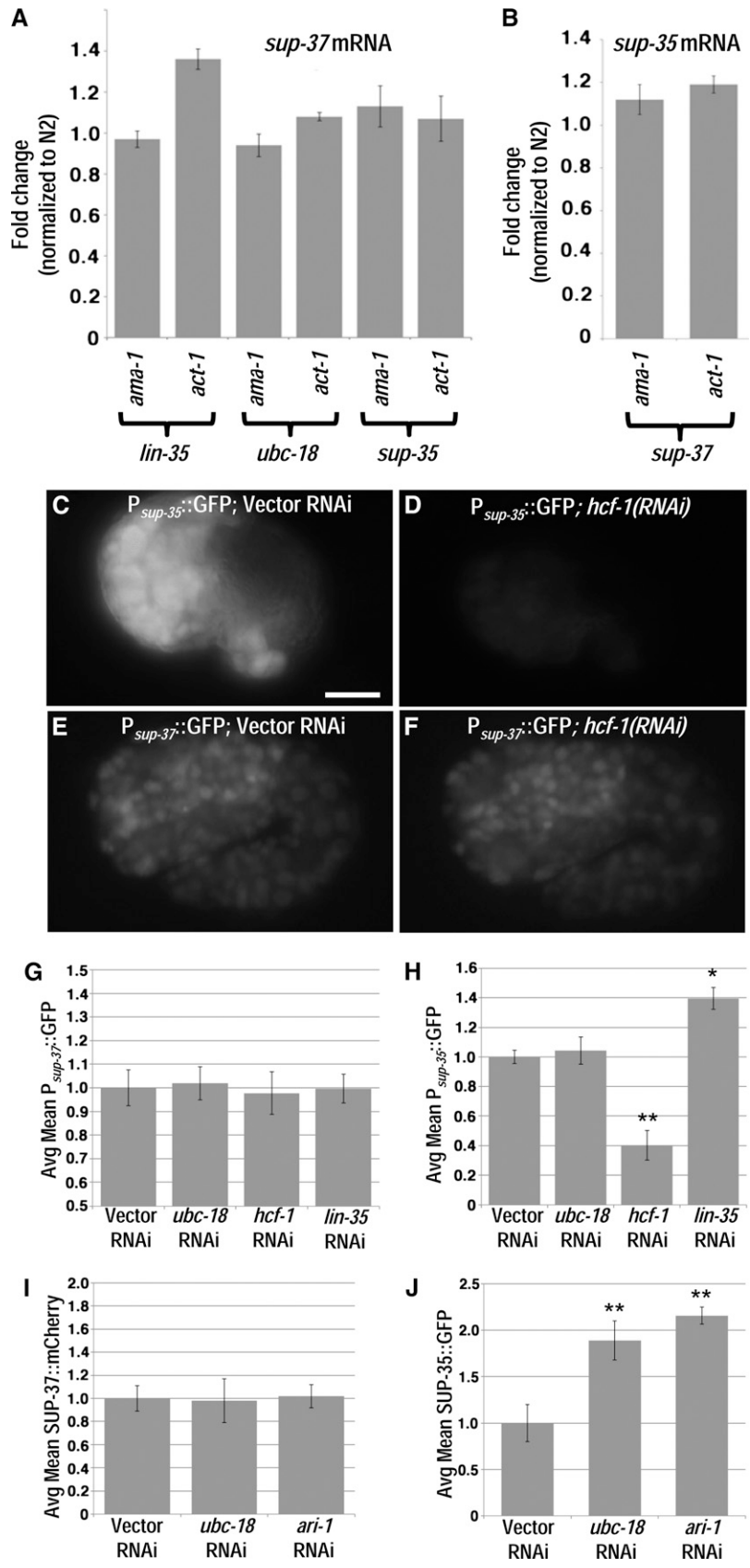


**Figure 8** Regulation of *sup-35* and *sup-37* expression. (A) Quantification of *sup-37* transcript levels by qRT-PCR in mutant backgrounds relative to wild type using two different internal controls. Mutations in *lin-35*(*n745*), *ubc-18* (*ku354*) and *sup-35*(*tm1810*) have no effect on *sup-37* mRNA levels. (B) Quantification of *sup-35* transcript levels by qRT-PCR in *sup-37*(*e2215*) mutants using two different internal controls. *sup-35* levels are not affected in *sup-37* single mutants. Representative fluorescence images of P<sub>sup-35</sub>::GFP (C and D) and P<sub>sup-37</sub>::GFP (E and F) embryos treated with vector control (C and E) and *hcf-1*(RNAi) (D and F). Bar in C, 10  $\mu$ m in C-F. (G and H) Quantification of P<sub>sup-35</sub>::GFP (G), P<sub>sup-37</sub>::GFP (H), SUP-37::mCherry (I), and SUP-35::GFP (J) mean fluorescence intensity of RNAi-treated embryos relative to vector RNAi control. Error bars indicate SEM. \*P < 0.05; \*\*P < 0.01.

**Table 4** Suppression of *pha-1* deletion mutants

Genotype	Suppression
<i>pha-1(tm3569)</i> ; control (RNAi)	No
<i>pha-1(tm3569)</i> ; <i>sup-35</i> (RNAi)	Yes
<i>pha-1(tm3569)</i> ; <i>sup-35</i> (RNAi); <i>pha-1</i> (RNAi)	Yes
<i>pha-1(tm3671)</i> ; control (RNAi)	No
<i>pha-1(tm3671)</i> ; <i>sup-35</i> (RNAi)	Yes
<i>pha-1(tm3671)</i> ; <i>sup-35</i> (RNAi); <i>pha-1</i> (RNAi)	Yes
<i>pha-1(tm3569)</i> ; <i>sup-37(e2215)</i>	No
<i>pha-1(tm3569)</i> ; <i>sup-37(tm356)</i>	Yes
<i>pha-1(tm3569)</i> ; <i>sup-37(tm356)</i> ; <i>pha-1</i> (RNAi)	Yes
<i>pha-1(tm3569)</i> ; <i>sup-37(tm1083)</i>	Yes
<i>pha-1(tm3569)</i> ; <i>sup-37(tm1083)</i> ; <i>pha-1</i> (RNAi)	Yes
<i>pha-1(tm3671)</i> ; <i>sup-37(e2215)</i>	No
<i>pha-1(tm3671)</i> ; <i>sup-37(tm356)</i>	Yes
<i>pha-1(tm3671)</i> ; <i>sup-37(tm356)</i> ; <i>pha-1</i> (RNAi)	Yes
<i>pha-1(tm3671)</i> ; <i>sup-37(tm1083)</i>	Yes
<i>pha-1(tm3671)</i> ; <i>sup-37(tm1083)</i> ; <i>pha-1</i> (RNAi)	Yes

All experiments were carried out at 20°. Yes, suppression of *pha-1* embryonic and larval defects was observed in animals of that genotype. Suppressed worms do not display *pha-1*-associated defects but arrest at the L1 stage due to the absence of *sup-37* function.

absence of *sup-37* activity. Additionally, RNAi of *pha-1* did not disrupt the ability of the *sup-37* null mutants to suppress the *pha-1* deletions. Failure of the *sup-37* missense allele to suppress the *pha-1* null deletions indicates that the strength of *sup-37* loss-of-function mutations and their corresponding

ability to suppress *pha-1* loss-of-function alleles is correlated. This is also consistent with the relatively modest effects on PHA-1 expression observed in the *sup-37* hypomorphic mutant background vs. the *sup-35* null deletion (Figure 9).

Taken together, our findings indicate that, although SUP-35 and SUP-37 can negatively regulate *pha-1* expression, *pha-1* transcriptional derepression cannot account for the ability of *sup-35* and *sup-37* mutations to suppress *pha-1* loss of function. This conclusion is further supported by our finding that treatment conditions in which *sup-35*(RNAi) leads to only a modest increase in the expression of the *P<sub>pha-1</sub>::GFP* reporter (~1.2-fold), nevertheless still efficiently allow suppression of *pha-1(e2123ts)* lethality at 25° (data not shown). Furthermore, we find that the discrepancy between the ability of *sup-35*(RNAi) to suppress *pha-1* null mutations and the inability of deleted *sup-35* to suppress homozygous *tDf2* embryos can be explained by the presence of maternal *sup-35* in the progeny of the balanced *tDf2*/+ strain. Specifically, whereas *tDf2*/+ heterozygotes placed on vector-control RNAi segregate 24.3% lethal *pha-1*-like embryos and 0.1% arrested larvae ( $n = 572$ ), *tDf2*/+ placed on *sup-35*(RNAi) segregate 2.7% lethal embryos and 20.5% arrested L1 larvae ( $n = 526$ ). These results demonstrate that depletion of maternal *sup-35* is sufficient to bypass the *pha-1*-like embryonic arrest phenotype of *tDf2/tDf2*

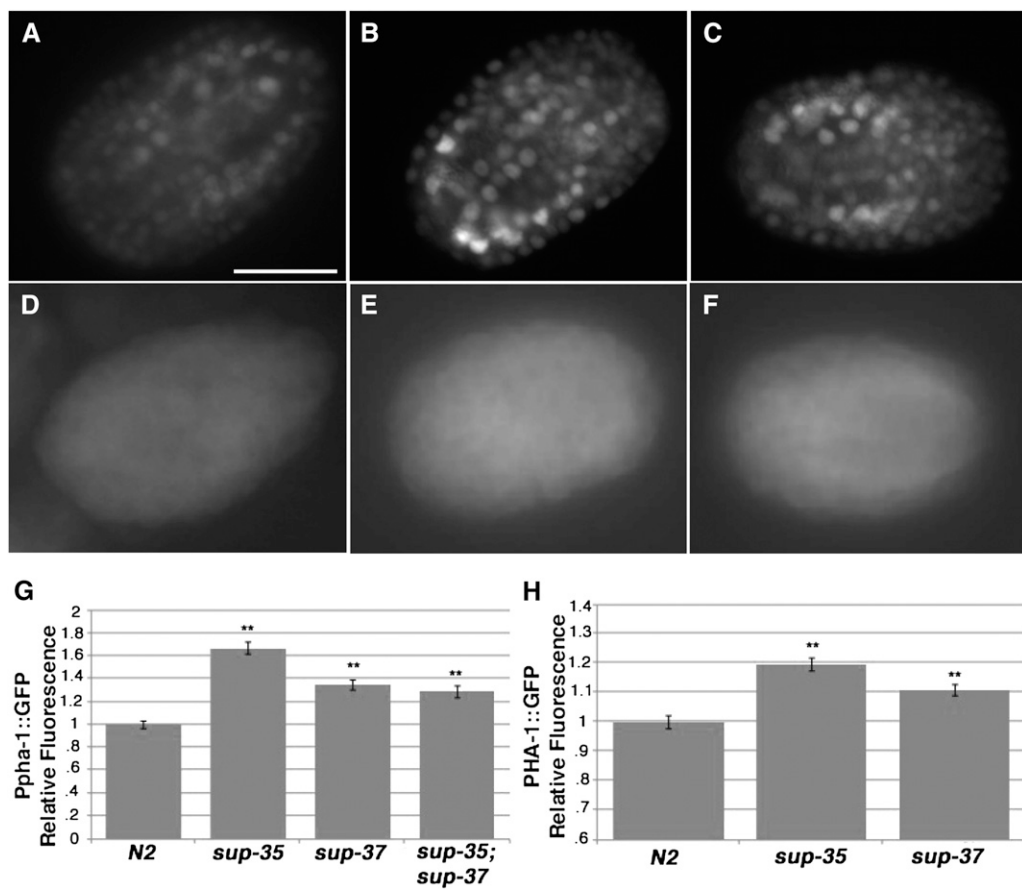


**Figure 9** SUP-37 and SUP-35 negatively regulate *pha-1* expression. Representative fluorescent images of *P<sub>pha-1</sub>::GFP* (A–C) and *PHA-1::GFP* (D–F) embryonic expression in N2 (A and D), *sup-35* (*tm1810*) (B and E), and *sup-37* (*e2215*) (C and F) mutants. Quantification of *P<sub>pha-1</sub>::GFP* (G) and *PHA-1::GFP* (H) fluorescence from A–F. In addition, *P<sub>pha-1</sub>::GFP* levels in *sup-35*; *sup-37* double mutants are shown in G. Error bars indicate SEM. \*\* $P < 0.01$ . Bar in A, 10  $\mu$ m in A–F.

homozygotes. The presence of arrested *tDf2/tDf2* larvae, which do not display pharyngeal defects, is presumably due to the zygotic absence of one or more additional genes within the *tDf2* region. Our finding that maternal *sup-35* is sufficient to preclude suppression of *pha-1* null mutants is also consistent with previous results showing that *sup-35* has a maternal component (Schnabel *et al.* 1991; Mani and Fay 2009). However, whereas loss of maternal or zygotic *sup-35* can suppress *pha-1* hypomorphic mutations (Schnabel *et al.* 1991), loss of both maternal and zygotic *sup-35* is apparently required for suppression of *pha-1* nulls. In summary, we conclude that loss of *sup-35* or *sup-37* activity can efficiently suppress the null phenotype of *pha-1* and that transcriptional derepression of *pha-1* in *sup-35* and *sup-37* mutants must therefore play a minor role at most in the observed genetic suppression.

## Discussion

On the basis of our findings described above, we propose the following working model (Figure 10). **PHA-1** promotes pharyngeal development and embryonic morphogenesis either by directly inhibiting the activities of **SUP-35/36/37** or through an indirect mechanism that somehow antagonizes the function of **SUP-35/36/37**. **SUP-35/36/37** in turn antagonizes pharyngeal development in part by inhibiting *pha-1* expression, but most importantly by acting through a distinct downstream target. Because **SUP-35** and **SUP-37** contain Zn fingers and can reside in the nucleus, the most likely function of **SUP-35/36/37** involves transcriptional regulation. Given that **PHA-1** is constitutively cytoplasmic, whereas **SUP-35** translocates from the cytoplasm to the nucleus at the time of pharyngeal morphogenesis, it is possible that **PHA-1** regulates the timing of **SUP-35/36/37** translocation to the nucleus. In this model, unregulated access of **SUP-35/36/37** to the nuclear compartment may lead to changes in transcription that are deleterious to embryonic development. We note, however, that we have not observed obvious effects of **PHA-1** activity on the timing of **SUP-35** translocation (D. S. Fay and S. R. G. Polley, unpublished data). Thus, **PHA-1** may regulate the nuclear localization of **SUP-36** or **SUP-37**, or may act through a different mechanism to regulate **SUP-35/36/37** activity. Assaying for physical interactions between **PHA-1** and **SUP-35/36/37** as well as studies to determine whether **PHA-1** plays a role in the timing of **SUP-35/36/37** subcellular localization will be a focus of future efforts.

Although **SUP-35** and **SUP-37** appear to act at a common step to regulate pharyngeal development, we note several important differences. Unlike **SUP-35**, overexpression of **SUP-37** was not toxic in a wild-type background. Thus, if **SUP-35** and **SUP-37** were to function as components of a transcriptional regulatory complex, **SUP-35** may be stoichiometrically limiting. Also in contrast to *sup-35*, *sup-37* expression was not regulated by E2F-associated factors such as **LIN-35/pRb** and **HCF-1** (Figure 8). Consistent with this,

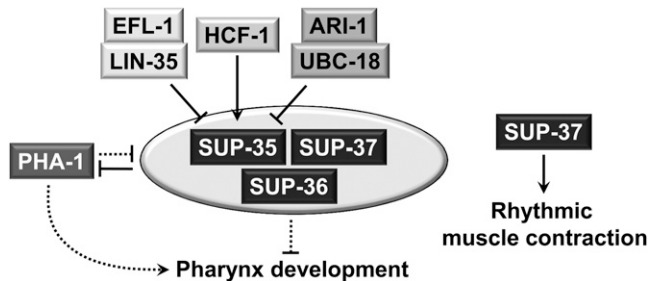


**Figure 10** Model for the **SUP-35–SUP-37** pathway controlling pharyngeal development.

**sup-37** upstream regulatory sequences do not contain consensus binding sites for E2F family members; nor have we previously detected alterations in **sup-37** mRNA levels in **lin-35** microarray experiments (Kirienko and Fay 2007). In addition, **sup-37** mRNA and **SUP-37** protein levels were not affected by inhibition of **UBC-18–ARI-1** activity, further suggesting that, unlike **sup-35**, **sup-37** is not a common target of the **LIN-35–EFL-1** and **UBC-18–ARI-1** pathways.

**SUP-37** also differs from **SUP-35** in that it carries out essential postembryonic functions. Our evidence implicates **SUP-37** within a small subset of pharyngeal muscle cell groups, termed **pm3** and **pm4**, to facilitate normal pumping in L1 larvae. The specific requirement within these cells, however, appears to be somewhat flexible. Furthermore, **SUP-37** must be present in at least some **pm3** and **pm4** cells for normal pumping to occur. The slow rate of contraction of the **terminal bulb** in the *sup-37* mutant is interesting with respect to the failure of the **corpus** to contract. It is thought that the **corpus** is the source of a pharyngeal pacemaker that involves a pair of neurons, **MCL** and **MCR**. These neurons, however, cannot be the foci of *sup-37*, because they descend from **ABA**, not from **MS**, and the *sup-37* feeding defect is worse than that which follows ablation of these neurons (Avery and Horvitz 1989). We speculate that source of the pacemaker, although it requires the **MC** neurons, might be the rhythmic contractions of the **corpus** itself, and when they are impaired, the **terminal bulb** may undergo slow, default contractions.

In addition to pharyngeal pumping, **SUP-37** is also required in the **somatic gonad** to promote ovulation. These functions suggest that **SUP-37** may play a more general role in the regulation of myoepithelial tissues. Consistent with this, a role for **SUP-37** in muscle development or function was previously suggested by a genome-wide bioinformatical analysis of *cis*-regulatory elements that are active in muscle cells (Zhao *et al.* 2007). The mosaic analysis also raised the possibility that *sup-37* has a nonessential function in the intestine. Notably, the **intestine**, the **pharynx**, and the **somatic gonad** share a common feature, rhythmic contractions, that are achieved via electrical coupling (Avery and Thomas 1997; McCarter *et al.* 1999; Nehrke *et al.* 2008; Altun *et al.* 2002–2010). Taken together, our data suggest that **SUP-37** may play a role in promoting rhythmic contractions within an organ.

Several pieces of data also indicate that the muscle-specific functions of **SUP-37** are independent of its role in regulating pharynx development with **SUP-35** and **PHA-1**: (1) *sup-35* null mutants are not defective in pharyngeal pumping or ovulation (Mani and Fay 2009); (2) overexpression of **PHA-1** via extrachromosomal arrays does not lead to pharyngeal pumping or ovulation defects (Granato *et al.* 1994b); and (3) inactivation of *pha-1* after embryogenesis, using a temperature-sensitive allele, does not lead to feeding or fertility defects (Schnabel and Schnabel 1990; Granato *et al.* 1994a; Fay *et al.* 2004).

We also note that several other reports suggest additional biological roles for **SUP-37**. A genome-wide RNAi screen identified a clone corresponding to *sup-37* as one of seven genes that are synthetically lethal in combination with loss of *rap-1*, which encodes a conserved small GTPase (Frische *et al.* 2007). We note that we have verified this genetic interaction but did not observe pharyngeal defects in *rap-1(tm861)*; *sup-37(RNAi)* mutants, nor does *rap-1(RNAi)* suppress *pha-1(e2123ts)* defects (D. S. Fay, unpublished observations). Thus, the functional overlap of **SUP-37** and **RAP-1** does not appear to be relevant to the role of **SUP-37** in pharyngeal development. In addition, a study using chromatin-immunoprecipitation methods to identify **DAF-16** targets indicates that **SUP-37** may be a direct target for regulation by the **DAF-2/IGF-DAF-16/FOXO** pathway (Oh *et al.* 2006). Consistent with this, the *sup-37* genomic locus contains three consensus binding sites for **DAF-16**, and reduced *sup-37* activity leads to a shortened lifespan and enhanced dauer formation. Thus, **SUP-37** may control a set of diverse biological processes in addition to its roles in regulating pharyngeal development and function.

## Acknowledgments

We thank Amy Fluet for editing, and Stuart Kim, Ralf Schnabel, and the *Caenorhabditis* Genetics Center for providing strains. This work was supported by grant GM066868 from the National Institutes of Health. A. Kuzmanov was supported by Wyoming iDeA Networks of Biomedical Research Excellence GM103432.

## Literature Cited

- Ahringer, J., 2005 Reverse genetics (April 6, 2006), *WormBook*, ed. The *C. elegans* Research Community WormBook, doi/10.1895/wormbook.1.47.1, <http://www.wormbook.org>.
- Albertson, D. G., and J. N. Thomson, 1976 The pharynx of *Caenorhabditis elegans*. *Philos. Trans. R. Soc. Lond. B Biol. Sci.* 275: 299–325.
- Altun, Z. F., L. A. Herndon, C. Crocker, R. Lints and D. H. Hall, (eds) 2002–2010 *WormAtlas*, pp.
- Avery, L., and H. R. Horvitz, 1989 Pharyngeal pumping continues after laser killing of the pharyngeal nervous system of *C. elegans*. *Neuron* 3: 473–485.
- Avery, L., and J. H. Thomas, 1997 Feeding and Defecation, pp. 679–716 in *C. elegans II*, edited by D. L. Riddle, T. Blumenthal, B. J. Meyer, and J. R. Priess. Cold Spring Harbor Laboratory Press, Cold Spring Harbor, NY.
- Edgley, M., A. D’Souza, G. Moulder, S. McKay, B. Shen *et al.*, 2002 Improved detection of small deletions in complex pools of DNA. *Nucleic Acids Res.* 30: e52.
- Fay, D., 2006 Genetic mapping and manipulation: chapter 5-SNPs: three-point mapping (February 17, 2006), *WormBook*, ed. The *C. elegans* Research Community WormBook, doi/10.1895/wormbook.1.94.1, <http://www.wormbook.org>.
- Fay, D. S., and J. Yochem, 2007 The SynMuv genes of *Caenorhabditis elegans* in vulval development and beyond. *Dev. Biol.* 306: 1–9.
- Fay, D. S., E. Large, M. Han, and M. Darland, 2003 lin-35/Rb and ubc-18, an E2 ubiquitin-conjugating enzyme, function redundantly to control pharyngeal morphogenesis in *C. elegans*. *Development* 130: 3319–3330.
- Fay, D. S., X. Qiu, E. Large, C. P. Smith, S. Mango *et al.*, 2004 The coordinate regulation of pharyngeal development in *C. elegans* by lin-35/Rb, pha-1, and ubc-18. *Dev. Biol.* 271: 11–25.
- Frische, E. W., W. Pellis-van Berkel, G. van Haaften, E. Cuppen, R. H. Plasterk *et al.*, 2007 RAP-1 and the RAL-1/exocyst pathway coordinate hypodermal cell organization in *Caenorhabditis elegans*. *EMBO J.* 26: 5083–5092.
- Granato, M., H. Schnabel, and R. Schnabel, 1994a Genesis of an organ: molecular analysis of the *pha-1* gene. *Development* 120: 3005–3017.
- Granato, M., H. Schnabel, and R. Schnabel, 1994b *pha-1*, a selectable marker for gene transfer in *C. elegans*. *Nucleic Acids Res.* 22: 1762–1763.
- Greenstein, D., 2005 Control of oocyte meiotic maturation and fertilization (December 28, 2005), *WormBook*, ed. The *C. elegans* Research Community WormBook, doi/10.1895/wormbook.1.53.1, <http://www.wormbook.org>.
- Kirienko, N. V., and D. S. Fay, 2007 Transcriptome profiling of the *C. elegans* Rb ortholog reveals diverse developmental roles. *Dev. Biol.* 305: 674–684.
- Labrousse, A., S. Chauvet, C. Couillault, C. L. Kurz, and J. J. Ewbank, 2000 *Caenorhabditis elegans* is a model host for *Salmonella typhimurium*. *Curr. Biol.* 10: 1543–1545.
- Liu, X., F. Long, H. Peng, S. J. Aerni, M. Jiang *et al.*, 2009 Analysis of cell fate from single-cell gene expression profiles in *C. elegans*. *Cell* 139: 623–633.
- Mango, S. E., 2007 The *C. elegans* pharynx: a model for organogenesis (January 22, 2007), *WormBook*, ed. The *C. elegans* Research Community WormBook, doi/10.1895/wormbook.1.129.1, <http://www.wormbook.org>.
- Mango, S. E., 2009 The molecular basis of organ formation: insights from the *C. elegans* foregut. *Annu. Rev. Cell Dev. Biol.* 25: 597–628.
- Mani, K., and D. S. Fay, 2009 A mechanistic basis for the coordinated regulation of pharyngeal morphogenesis in *Caenorhabditis elegans* by LIN-35/Rb and UBC-18-ARI-1. *PLoS Genet.* 5: e1000510.
- McCarter, J., B. Bartlett, T. Dang, and T. Schedl, 1999 On the control of oocyte meiotic maturation and ovulation in *Caenorhabditis elegans*. *Dev. Biol.* 205: 111–128.
- Nehrke, K., J. Denton, and W. Mowrey, 2008 Intestinal Ca<sup>2+</sup> wave dynamics in freely moving *C. elegans* coordinate execution of a rhythmic motor program. *Am. J. Physiol. Cell Physiol.* 294: C333–C344.
- Oh, S. W., A. Mukhopadhyay, B. L. Dixit, T. Raha, M. R. Green *et al.*, 2006 Identification of direct DAF-16 targets controlling longevity, metabolism and diapause by chromatin immunoprecipitation. *Nat. Genet.* 38: 251–257.

- Portereiko, M. F., and S. E. Mango, 2001 Early morphogenesis of the *Caenorhabditis elegans* pharynx. *Dev. Biol.* 233: 482–494.
- Portereiko, M. F., J. Saam, and S. E. Mango, 2004 ZEN-4/MKLP1 is required to polarize the foregut epithelium. *Curr. Biol.* 14: 932–941.
- Qiu, X., and D. S. Fay, 2006 ARI-1, an RBR family ubiquitin-ligase, functions with UBC-18 to regulate pharyngeal development in *C. elegans*. *Dev. Biol.* 291: 239–252.
- Schnabel, H., and R. Schnabel, 1990 An organ-specific differentiation gene, pha-1, from *Caenorhabditis elegans*. *Science* 250: 686–688.
- Schnabel, H., G. Bauer, and R. Schnabel, 1991 Suppressors of the organ-specific differentiation gene pha-1 of *Caenorhabditis elegans*. *Genetics* 129: 69–77.
- Schroeder, L. K., S. Kremer, M. J. Kramer, E. Currie, E. Kwan *et al.*, 2007 Function of the *Caenorhabditis elegans* ABC transporter PGP-2 in the biogenesis of a lysosome-related fat storage organelle. *Mol. Biol. Cell* 18: 995–1008.
- Stiernagle, T., 2005 Maintenance of *C. elegans* (February 11, 2006), *WormBook*, ed. The *C. elegans* Research Community WormBook, doi/10.1895/wormbook.1.101.1, <http://www.wormbook.org>.
- Sulston, J. E., E. Schierenberg, J. G. White, and J. N. Thomson, 1983 The embryonic cell lineage of the nematode *Caenorhabditis elegans*. *Dev. Biol.* 100: 64–119.
- van den Heuvel, S., and N. J. Dyson, 2008 Conserved functions of the pRB and E2F families. *Nat. Rev. Mol. Cell Biol.* 9: 713–724.
- Yochem, J., T. Gu, and M. Han, 1998 A new marker for mosaic analysis in *Caenorhabditis elegans* indicates a fusion between hyp6 and hyp7, two major components of the hypodermis. *Genetics* 149: 1323–1334.
- Zhao, G., L. A. Schriever, and G. D. Stormo, 2007 Identification of muscle-specific regulatory modules in *Caenorhabditis elegans*. *Genome Res.* 17: 348–357.

Communicating editor: K. Kemphues

# GENETICS

Supporting Information

<http://www.genetics.org/content/suppl/2012/04/27/genetics.112.140814.DC1>

## A Regulatory Module Controlling Pharyngeal Development and Function in *Caenorhabditis elegans*

David S. Fay, Stanley R. G. Polley, Jujiao Kuang, Aleksandra Kuzmanov, James W. Hazel,  
Kumaran Mani, Bethany L. Veo, and John Yochem

### Isoform A

## Isoform B

### Isoform C

### Isoform D

ATGAGCATCAGCGGAGAGGACAACGAGATTACTGAACGCAAGTCTATCAAATTCTCCGACCAGTTAGACGTTTTGAGGAAAGTCGTGAAATT  
TTCTCGAGAGTATCACGCAACAGtttgttttatattaaatataacgtttctgqaaacatcttggaaatgtttaaattqaaaacta

Shaded yellow regions indicate locations of exons.

## **Figure S1 sup-37/ztf-12 isoforms.**

### **Amino acid sequence of C01B7.1a**

MSISGEDNEI ILNASLSNSP DQLDVFEESR RNFLESINAT VSMTSNGSKN GIEDIANRLK QNGNTTSTSL  
TSNSGLYPTD PTIISNHTPS MQLSCVECGV TKANSEEMEI HIKTEHLKWL PFQCPMCLVE RASDAQMREH  
LHSSHQKNMS KFIYVDNVKA KRRLQILMDS AFSLNVSERV NAKNHPSSST SASPYSPSY HRGMNSSPSS  
GRNTSTSNGS ATSAATASAQ AAATAIVNHH KEKEKQTAQA TADFLKLDF TGINGEIGEH KAQSSTRSS  
SGRKRPYVPT SATEAITTME LAAPSAESFL ASLNSFSHAQ TPENEENDHP TLFSVDDLNI DSTSTLATLF  
GGGARKTKYD DGEMPHDEDP LLDSLNPISV LDNVAALFGS TPDRSVETET KKTSSISKKR VLGECSKCQK  
PVTAGARQMH MFFHLAKDEL IFRFRCKHEG CSVEHYRKDQ MENHQSKAHG RIDPDMMEDR SLELFOKCQE  
LNHELPVAHR HGHRASPQWT GGSADLAGYQ NSQKSCLPGL SSLCSSTAGT AGSTSNGFGP LKLPVDEDHP  
LQCRLCGKTM QNRIRGFHIL WHMAKDKGIN RYTCKYCNFG HDRSQSVQVH GKKEHGTDDC VEDRIGEYQD  
DVKE<sup>M</sup>SASC<sup>F</sup> GISSLFAQES KRKNKFPAAA PREHKDLVSM VSSSHEASPA VPVDEEASND SAIKEEKPL  
ILNDEEMEE<sup>L</sup> GEDDEVEHEQ EHEDEDGEGD EDDDGEGEET TPITSSKSSK KKWRRAFNIR SKKSKKQKED  
AVVARVS<sup>S</sup>SIL IGGAQFYKKK VNEFCYCEKC GKQTN<sup>S</sup>R<sup>L</sup>P<sup>E</sup> HAYTHMDGVE LYSCSACSF<sup>G</sup> NQCKETVMKH  
MRESHPLCAE RCVDNRLGHI KEIKKQLGQC FPAFFIDHPL PTRSDIEKLQ ILASGGDLKI GGIEKYLKEE  
CEDGEPE<sup>S</sup>AP EDEEMEEDDDGVSSD

### **Amino acid sequence of allele *tm356***

MSISGEDNEI ILNASLSNSP DQLDVFEESR RNFLESINAT VSMTSNGSKN GIEDIANRLK QNGNTTSTSL  
TSNSGLYPTD PTIISNHTPS MQLSCVECGV TKANSEEMEI HIKTEHLKWL PFQCPMCLVE RASDAQMREH  
LHSSHQKNMS KFIYVDNVKA KRRLQILMDS AFSLNVSERV NAKNHPSSST SASPYSPSY HRGMNSSPSS  
GRNTSTSNGS ATSAATASAQ AAATAIVNHH KEKEKQTAQA TADFLKLDF TGINGEIGEH KAQSSTRSS  
SGRKRPYVPT SATEAITTME LAAPSAESFL ASLNSFSHAQ TPENEENDHP TLFSVDDLNI DSTSTLATLF  
GGGARKTKYD DGEMPHDEDP LLDSLNPISV LDNVAALFGS TPDRSVETET KKTSSISKKR VLGECSKCQK  
PVTAGARQMH MFFHLAKDEL IFRFRCKHEG CSVEHYRKDQ MENHQSKAHG RIHKSRNFPD CQVFALQPQA  
LLVALQT<sup>V</sup>S<sup>D</sup> L

### **Amino acid sequence of allele *tm1083***

MSISGEDNEI ILNASLSNSP DQLDVFEESR RNFLESINAT VSMTSNGSKN GIEDIANRLK QNGNTTSTSL  
TSNSGLYPTD PTIISNHNEE NDHPTLFSVD DLNIDSTSTL ATLF<sup>G</sup>GGARK TKYDDGEMPH DEDPLLD<sup>S</sup>LN  
PISVL<sup>D</sup>NVA<sup>A</sup> LFGSTPDR<sup>S</sup>V ETETKKTSSI SKKRVLGECS KCQKPV<sup>T</sup>AGA RQHM<sup>M</sup>F<sup>H</sup>LA KDELIFRFRC  
KHEGCSVEHY RKDQMENHQ<sup>S</sup> KAHGRIDPDM MEDRSLELFQ KCQE<sup>I</sup>NHELP VAHRHGRAS PQWTGGSADL  
AGYQNSQKSK LPGLSSLC<sup>S</sup> TAGTAG<sup>S</sup>SN GFGPLKLPD EDHPLQCRLC GKT<sup>M</sup>QNRIRG F<sup>H</sup>ILWHMAKD  
KG<sup>I</sup>NR<sup>Y</sup>TCKY CNFGHDR<sup>S</sup>QS VQVHGKKEH<sup>G</sup> TDDCVEDRIG EYQDDVKEMS ASCFGISSLF AQESKRKNKF  
PAAAPREHKD LVSMVSS<sup>S</sup>HE ASPAVPV<sup>D</sup>EE ASND<sup>S</sup>AIKEE EKPLILN<sup>D</sup>EE MEELGEDDEV EHEQEHEDED  
GEGDEDDDG<sup>E</sup> GEETTPIT<sup>S</sup>S KSSKKWRR<sup>A</sup> FNIRS<sup>K</sup>SK<sup>K</sup>K KEDAVVARS VSILIGGAQF YKKVNEFCY  
CEKCGKQTNS RLPEHAYTHM DGVELYSCSA CSFGNQCKET VMKHMRESHP LCAERCVDNR LGHIKEIKKQ  
LGQCFPAFFI DHPLPTRSDI EKLQILASGG DLKIGGIEKY LKEECEDEME EDDDG<sup>V</sup>SSD

**XXXXX** - predicted Zn fingers

**XXXXX** - region deleted in *tm356*

**x** - insertion

**XXXXX** - region deleted in *tm1083*

**x** - missense mutations

**Figure S2 Amino acid sequences of wild-type and mutant forms of SUP-37/ZTF-12.**

*Ce*, *C. elegans*; *Cre*, *C. remanei*; *Cbr*, *C. briggsae*. *Cre\_ztf-12* is also annotated as CRE05800, *Cbg\_ztf-12* as CBG00762. Asterisks indicate identity in all three species; colons, identity in two species with similarity in one species; periods, identity in two species with no similarity in third species. Red shading indicates locations of point mutations. Yellow shading indicates locations of zinc-finger domains (ZF1-ZF7).

**Figure S3** Alignment of SUP-37/ZTF-12 orthologs in *Caenorhabditis* species.